BARD Final Report IS-4764-14R

Optimization of advanced greenhouse substrates based on physicochemical characterization, numerical simulations, and tomato growth experiments

Tuller, M. Arizona Board of Regents, The University of Arizona AZ
Bar-Tal, A. Agricultural Research Organization
Heller, H. Agricultural Research Organization
Amichai, M. Ramat Negev Desert Agro-Research R&D

Project award year: 2014
Three year research project

Project Abstract – BARD-4764

Over the last decade there has been a dramatic shift in global agricultural practice. The increase in human population, especially in underdeveloped arid and semiarid regions of the world, poses unprecedented challenges to production of an adequate and economically feasible food supply to undernourished populations. Furthermore, the increased living standard in many industrial countries has created a strong demand for high-quality, out-of-season vegetables and fruits as well as for ornamentals such as cut and potted flowers and bedding plants. As a response to these imminent challenges and demands and because of a ban on methyl bromide fumigation of horticultural field soils, soilless greenhouse production systems are regaining increased worldwide attention. Though there is considerable recent empirical and theoretical research devoted to specific issues related to control and management of soilless culture production systems, a comprehensive approach that quantitatively considers all relevant physicochemical processes within the growth substrates is lacking. Moreover, it is common practice to treat soilless growth systems as static, ignoring dynamic changes of important physicochemical and hydraulic properties due to root and microbial growth that require adaptation of management practices throughout the growth period.

To overcome these shortcomings, the objectives of this project were to apply thorough physicochemical characterization of commonly used greenhouse substrates in conjunction with state-of-the-art numerical modeling (HYDRUS-3D, PARSWMS) to not only optimize management practices (i.e., irrigation frequency and rates, fertigation, container size and geometry, etc.), but to also “engineer” optimal substrates by mixing organic (e.g., coconut coir) and inorganic (e.g., perlite, pumice, etc.) base substrates and modifying relevant parameters such as the particle (aggregate) size distribution. To evaluate the proposed approach under commercial production conditions, characterization and modeling efforts were accompanied by greenhouse experiments with tomatoes.

The project not only yielded novel insights regarding favorable physicochemical properties of advanced greenhouse substrates, but also provided critically needed tools for control and management of containerized soilless production systems to provide a stress-free rhizosphere environment for optimal yields, while conserving valuable production resources. Numerical modeling results provided a more scientifically sound basis for the design of commercial greenhouse production trials and selection of adequate plant-specific substrates, thereby alleviating the risk of costly mistrials.

Summary Sheet

Publication Summary

PubType	IS only	Joint	US only
Abstract - Poster	0	4	0
Book Chapter	0	1	0

Training Summary

Trainee Type	Last Name	First Name	Institution	Country
Ph.D. Student	Gohardoust	Mohammad	University of Arizona	USA
Postdoctoral Fellow	Babaeian	Ebrahim	University of Arizona	USA

Collaborative Contributions – BARD-4764

The Israeli research group at the Volcani Center (Asher Bar-Tal, Hadar Heller, and Michal Amichai) performed 2 extensive greenhouse growth experiments at the Ramat Negev Desert Agro Research Center and provided plant and physicochemical data to the U.S. group (Ebrahim Babaeian, Mohammad Gohardoust and Markus Tuller) to develop the numerical HYDRUS model. The U.S. group performed extensive physicochemical characterization of soilless substrates (perlite, coconut coir, tuff, Growstones and mixtures thereof) that have been used to numerically model flow and transport processes in plant growth modules with HYDRUS 3D considering water and nutrient uptake of tomato plants. The U.S. group further adapted and modified the PARSWMS parallel code for modeling of flow and transport processes in the plant growth modules. Finally, the U.S. group developed a framework for estimation of the water characteristic of soilless substrate mixtures from the water characteristics of their constituents.

All members of both groups jointly worked on presentations at scientific meetings. Asher Bar-Tal and Markus Tuller also worked on a book chapter for the 2nd Edition of Soilless Culture: Theory and Practice to be published by Elsevier.

Both groups are currently working jointly on several refereed publications.

Final Project Report – BARD Award US-4764-14R

Optimization of Advanced Greenhouse Substrates Based on Physicochemical Characterization, Numerical Simulations, and Tomato Growth Experiments

Markus Tuller, Asher Bar-Tal, Hadar Heller, and Michal Amichai

Contact:
Markus Tuller
Professor of Environmental Physics
The University of Arizona
SWES Department
Shantz 38, Room 526
Tucson, AZ 85721-0038
Phone: (520) 621-7225
Email: mtuller@email.arizona.edu

SUMMARY OF ACHIEVEMENTS

- Extensive physicochemical characterization of soilless substrates (perlite, coconut coir, tuff, Growstones and mixtures thereof). **USA**

- Numerical modeling of flow and transport processes in plant growth modules with HYDRUS 3D considering water and nutrient uptake of tomato plants. **USA**

- Adaptation and modification of the PARSWMS parallel code for modeling of flow and transport processes in plant growth modules with high performance super computers considering plant water and nutrient uptake. **USA**

- Development of a framework for estimation of the water characteristic of soilless substrate mixtures from the water characteristics of their constituents. **USA**

- Tomato greenhouse growth experiments. **Israel**

We are currently working on several joint refereed publications.

1. Achievements - University of Arizona

1.1 Physicochemical Characterization of Soilless Substrates

The initially characterized substrates included volcanic tuff, horticultural perlite, coconut coir, a tuff/coconut coir mixture (70/30 vol.-%), a perlite/coconut coir mixture (50/50 vol.-%), and a foamed glass/coconut core mixture (50/50 vol.-%). To develop a framework for estimating the soil water characteristic (SWC) of substrate mixtures from the SWCs of the individual mixture constituents, additional measurements for perlite/coconut coir and tuff/coconut coir mixtures (25/75 vol.-%, 50/50 vol.-%, 75/25 vol.-%) were performed.

To obtain uniform and reproducible substrate samples for hydraulic characterization we first performed comprehensive compaction trials to determine the lowest and highest achievable dry bulk densities for the considered soilless substrates. The average dry bulk densities were then used as initial target bulk densities for preparation of core samples for soil water characteristic (SWC) and saturated hydraulic conductivity (Ksat) measurements. The Growstones/coir mixture supplied by Growstone, LLC to the Volcani Center and the UA was separated and remixed and homogenized at 50/50 vol.-% (it was not possible to collect homogeneous subsamples directly from the supplied material). All tests were performed in sextuplicate for each single substrate and all mixtures. Air-dry substrates were used as this is the most realistic scenario for large-scale greenhouse trials and also to avoid potential problems with hydrophobicity of oven-dry coconut coir.

Compaction Procedure for Uniform Substrates: Perlite, Tuff, and Coconut Coir

First, several subsamples of the air-dry substrates are collected and oven-dried to determine the "air-dry" gravimetric water content:

$$\theta_m = \frac{M_{AD} - M_{OD}}{M_{OD}}$$

where M_{AD} is the mass of the air-dry subsample and M_{OD} is the mass of the oven-dry subsample.

Then the thoroughly homogenized air-dry substrates are compacted into cylinders with known volume (V_C) and mass (M_C). To achieve a uniform packing density, the cylinders are divided into multiple layers (based on the size of the cylinder the number of sub-layers can vary). Then the substrate is added layer by layer.

To achieve the lowest potential packing density, the substrates are poured into and carefully distributed within the cylinders with the fingers without imposing any significant compaction force. Only on the very top the substrate particles are gently pushed inside the cylinder to obtain a smooth surface. To achieve the highest potential packing density, the substrates are compacted layer by layer with a rubber stopper mounted on a push rod. After compaction the mass of the cylinder and the air-dry sample $(M_{AD+C})$is determined and the dry bulk density calculated:

$$\rho_b = \frac{\left(\frac{M_{AD+C} - M_C}{1 + \theta_m}\right)}{V_c} = \frac{M_{OD}}{V_c}$$

The determined lowest and highest dry bulk densities and the average values are listed below in Table 1.

For preparation of samples for SWC and K_{sat} measurements the average dry bulk densities (Table 1) are used as target. The mass of air-dry substrate required to fill a distinct volume at the target bulk density is calculated as:

$$M_{AD} = \rho_b \times V \times (1 + \theta_m)$$

with ρ_b as the target dry bulk density, *V* the volume of container and θ_m the gravimetric water content of the air-dry substrate.

To achieve a uniform bulk density within the cylinders they are divided into multiple layers (based on the size of the container the number of sub-layers can vary). Then the substrate is added layer by layer.

Compaction Procedure for Mixtures

Compaction trials were performed for 50/50 vol.-% perlite/coir mixture, 70/30 vol.-% tuff/coir mixture, and 50/50 vol.-% Growstones/coir mixture. First, several subsamples of the individual substrates to be mixed are collected and oven-dried to determine the "air-dry" gravimetric water contents. *The Growstones/coir mixture supplied by Growstone, LLC to the Volcani Center and the UA was separated into single components.*

$$\theta_{m1} = \frac{M_{AD1} - M_{OD1}}{M_{OD1}} \qquad \theta_{m2} = \frac{M_{AD2} - M_{OD2}}{M_{OD2}}$$

where M_{AD} is the mass of the air-dry subsample and M_{OD} is the mass of the oven-dry subsample.

Once the gravimetric water contents of the individual mixture components are known, the substrates (S_1, S_2) are poured into two separate cylinders of known volumes (V_{C1}, V_{C2}) and carefully distributed within the fingers without imposing any significant compaction force. Only on the very top the substrate particles are gently pushed inside the cylinder to obtain a smooth surface. The air-dry mass of the substrates (M_{ADv1}, M_{ADv2}) occupying a specific volume is then measured and the oven-dry masses per volume (M_{ODv1}, M_{ODv2}) are calculated.

$$M_{ODv1} = \left(\frac{M_{ADv1}}{1 + \theta_{m1}}\right)\frac{1}{V_{C1}} \qquad M_{ODv2} = \left(\frac{M_{ADv2}}{1 + \theta_{m2}}\right)\frac{1}{V_{C2}}$$

Once the oven-dry masses per volume (M_{ODv1}, M_{ODv2}) the dry mass ratio $(\propto)$ is calculated as:

$$\propto = \frac{M_{ODv1}}{M_{ODv2}} \times R_V$$

where R_V is the volumetric substrate mixing ratio (i.e., 50/50 for perlite/coir; 70/30 for tuff/coir; and 50/50 for Growstones/coir). The obtained dry mass ratios are listed below in Table 2.

For the compaction trials the air-dry substrate components are then mixed at the desired volumetric substrate mixing ratio and the resulting mixture is meticulously homogenized (this can take some time). The homogenized air-dry mixture is than compacted into cylinders in the same fashion as for individual substrates.

To achieve the lowest potential packing density, the mixtures are poured into and carefully distributed within the cylinders with the fingers without imposing any significant compaction force. Only on the very top the substrate particles are gently pushed inside the cylinder to obtain a smooth surface.

To achieve the highest potential packing density, the mixtures are compacted layer by layer with a rubber stopper mounted on a push rod. After compaction the mass of the air-dry mixture occupying the cylinder (M_{ADmix}) is determined and the oven-dry masses of the individual components composing the sample (M_{OD1}, M_{OD2}) are calculated:

$$M_{OD2} = \frac{M_{ADmix}}{\left(\propto \left(\frac{1+\theta_{m1}}{1+\theta_{m2}}\right)+1\right)} \frac{1}{(1+\theta_{m2})}$$

$$M_{OD1} = \left(M_{ADmix} - \frac{M_{ADmix}}{\left(\propto \left(\frac{1+\theta_{m1}}{1+\theta_{m2}}\right)+1\right)}\right) \frac{1}{(1+\theta_{m1})}$$

Then the oven-dry mass of the mixture (M_{ODmix}) is calculated and divided by the cylinder volume (V_C) to yield the dry bulk density of the mixture (ρ_{b-mix}), which is used as target for subsequent SWC, Ksat, and gas diffusion experiments:

$$M_{ODmix} = M_{OD1} + M_{OD2}$$

$$\rho_{b-mix} = \frac{M_{ODmix}}{V_c}$$

The determined lowest and highest dry bulk densities and the average values are listed below in Table 1.

For preparation of mixture samples for SWC and K_{sat} measurements the average dry bulk densities (Table 1) are initially used as target. If time permits, all experiments will be also performed at the lowest and highest achievable dry bulk densities. The mass of air-dry substrate required to fill a distinct volume (V)at the target bulk density is calculated as:

$$M_{ADmix} = \left[\frac{1+\theta_{m1}}{1+\propto^{-1}} + \frac{1+\theta_{m2}}{1+\propto}\right] \times \rho_{b-mix} \times V$$

To achieve a uniform bulk density within the cylinders they are divided into multiple layers (based on the size of the container the number of sub-layers can vary). Then the homogenized mixture is added layer by layer.

Table 1. Dry bulk densities determined with compaction experiments

Substrate	Dry Bulk Density [g cm^{-3}]		
	Lowest	**Average**	Highest
Perlite	0.072	**0.076**	0.080
Coconut coir	0.100	**0.110**	0.120
Tuff	1.100	**1.150**	1.200
Perlite + Coir	0.082	**0.088**	0.094
Tuff + Coir	0.875	**0.925**	0.975
Growstones + Coir	0.180	**0.185**	0.190

Table 2. Oven-dry mass ratios of mixtures

Mixture	Mixing Ratio (vol.-%)	Oven-Dry Mass Ratio
Perlite/Coconut Coir	50/50	0.7282
Tuff/Coconut Coir	70/30	27.5247
Growstones/Coconut Coir	50/50	2.8946

1.1.1 Soil Water Characteristic (SWC)

Tempe cells were used to measure the wet-end of the SWC curve. The Tempe cells (Soilmoisture Equipment Corp., Santa Barbara, CA) were connected to a pressure manifold (Fig. 1) with a high-resolution pressure/vacuum regulator and initially saturated samples were sequentially desaturated by applying increasing pressures. Each pressure step was maintained until the sample was in equilibrium with the applied pressure and the outflow ceased. A detailed description of the pressure desaturation method is provided in Tuller and Or (2004).

Figure 1: Tempe cell experiments at the University of Arizona.

After completion of the measurements the van Genuchten (1980) and Durner (1994) SWC models were parameterized via nonlinear regression to measured data:

$$\theta = \theta_r + (\theta_s - \theta_r)\left[\frac{1}{1+(\alpha|\psi|)^n}\right]^m$$

$$\theta = \theta_r + (\theta_s - \theta_r)\left[(1-w)\left(\frac{1}{1+\alpha_1|\psi|^{n_1}}\right)^{m_1} + w\left(\frac{1}{1+\alpha_2|\psi|^{n_2}}\right)^{m_2}\right]$$

where θ is the volumetric water content, θ_r and θ_s are residual and saturated water content respectively, ψ is matric potential, and α, n, and m are shape parameters with $m = 1 - 1/n$. w is weighting factor which varies between 0 and 1. The van Genuchten parameters are listed in Table 3 and measurements together with the van Genuchten curves are depicted in Fig. 2.

Table 3. Parameters of the van Genuchten (1980) and Durner (1994) SWC models for investigated substrates

Substrate	θ_s	θ_r	α_1	n_1	α_1	n_1	w
Perlite	0.818	0.001	1.688	1.156	-	-	-
Tuff	0.483	0.014	2.006	1.262	-	-	-
Coconut coir	0.874	0.010	0.063	1.296	-	-	-
Perlite/Coconut coir	0.837	0.005	0.422	1.199	-	-	-
Tuff/Coconut coir	0.549	0.014	0.449	1.267	-	-	-
Growstone/Coconut coir	0.722	0.004	0.327	1.228	3.00	20	0.226

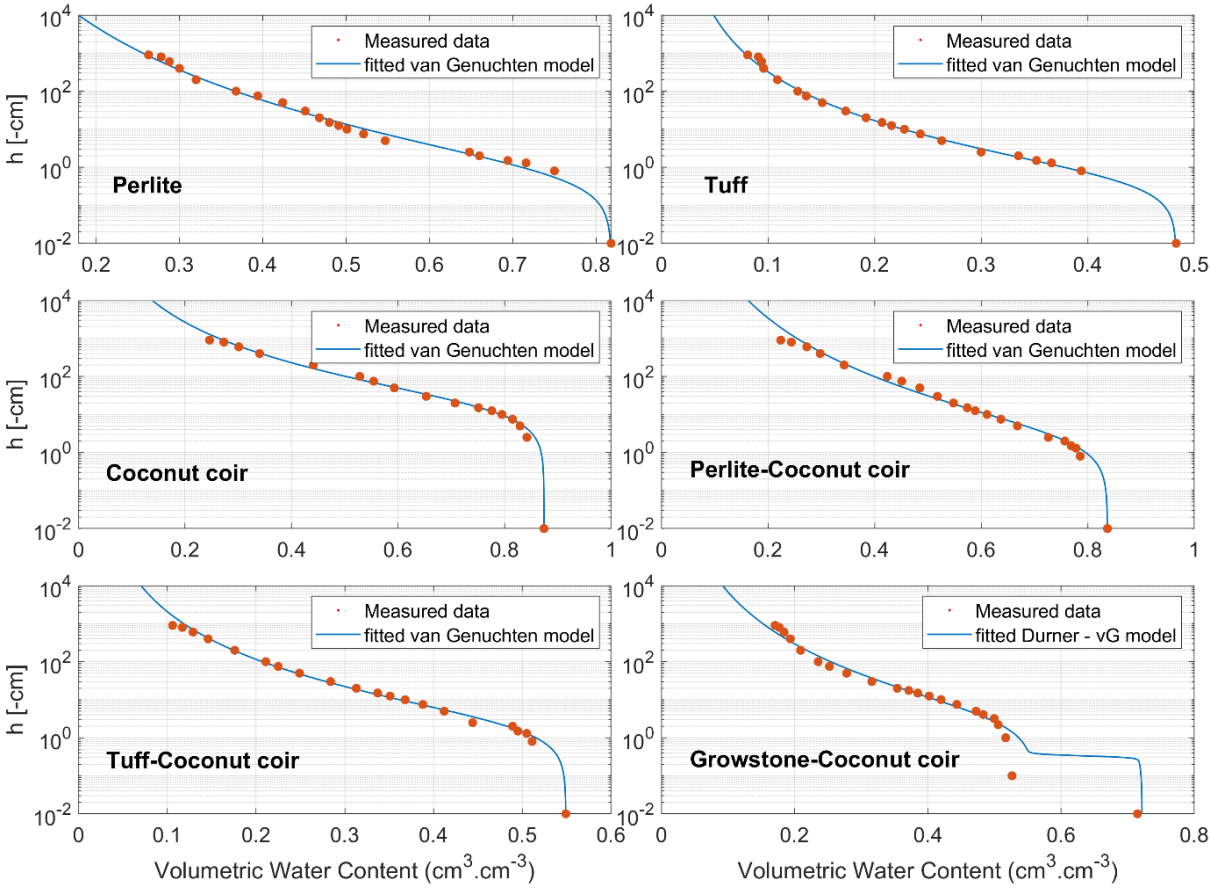

Figure 2: Measured SWC curves depicted with the parameterized van Genuchten (1980) and Durner (1994) models.

1.1.2 Saturated Hydraulic Conductivity (K_{sat})

For the K_{sat} measurements we designed and fabricated an automated constant head device placed on a load cell attached to a laboratory jack and connected to a flow cell filled with substrate (Fig.3). The load cell was connected to a datalogger to record and monitor the weight changes of the constant head container (i.e., Marriot tank) while water was flowing through the sample. In addition, the water temperature was continuously measured with a thermocouple and used to convert mass to volume change. Each substrate was compacted into the flow cell with the average target bulk densities listed in Table 1. Before slowly saturating samples with water from the Marriot tank, they were flushed with CO_2 for about 10 minutes at very low flow rate to enhance the saturation process. After sample saturation the constant head was adjusted with a lab jack and the experiment initiated. The experiment was terminated after several hours of steady state flow. Each sample was measured at 20, 15, 10, and 5-cm hydraulic heads. Darcy's law was applied to calculate K_{sat} from the measured water flux density and set hydraulic head (Reynolds et al., 2002). The average measured K_{sat} values are listed in Table 4.

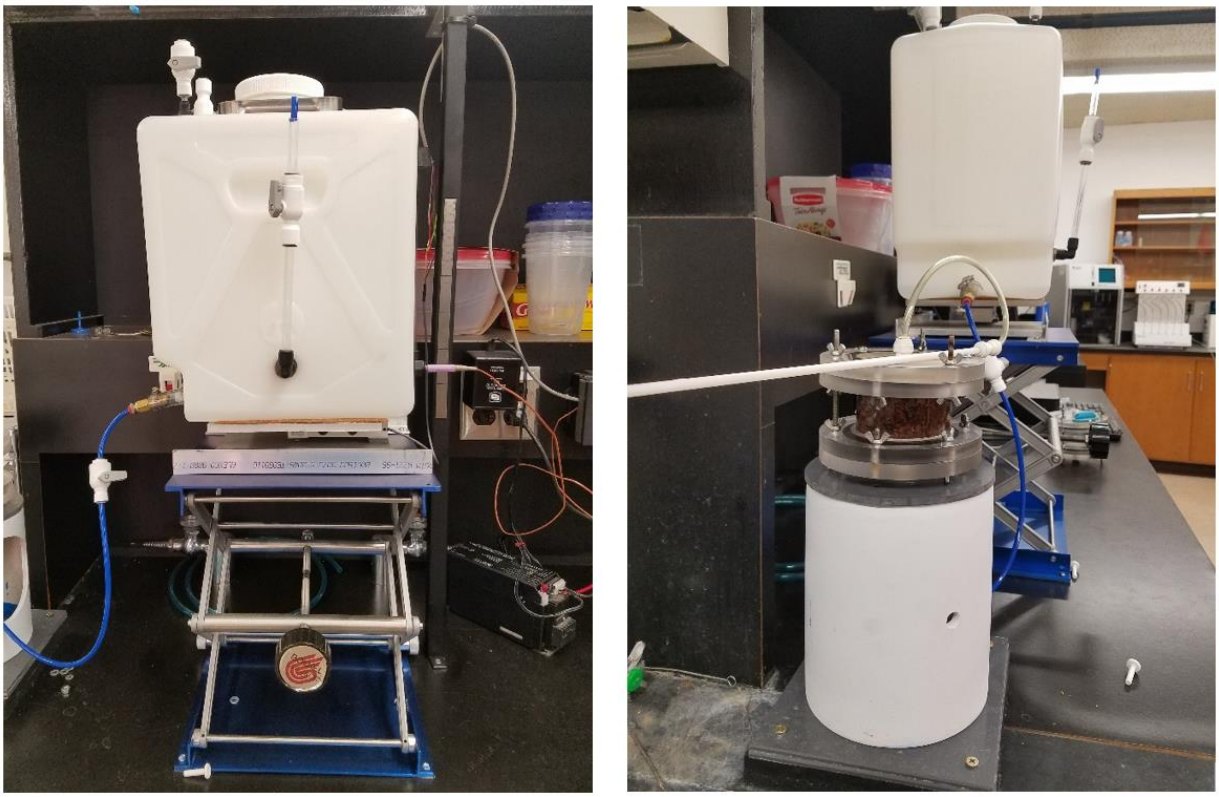

Figure 3: Automated constant head setup for K_{sat} measurements.

Table 4. Average saturated hydraulic conductivities measured with the constant head method

Substrate	K_{sat} (cm.d^{-1})
Perlite	7322
Tuff	7301
Coconut coir	1349
Perlite - Coconut coir	3962
Tuff - Coconut coir	2656
Growstone - Coconut coir	4139

1.1.3 Particle Density

While a standard water pycnometer was used to measure the particle densities of tuff and coconut coir, nitrogen gas pycnometry was applied for the lighter perlite and Growstone substrates. The densities of the mixtures can be simply calculated based on the volumetric mixing ratios. A Multipycnometer (Quantachrome Corp., Boynton Beach, FL) with nitrogen as probing gas was used for the latter measurements. To capture potential variability, 10 sub samples were measured for each substrate. Average particle density values are listed in Table 5.

Table 5. Average measured particle densities

Substrate	ρ (g cm^{-3})
Tuff	2.653
Coconut coir	1.717
Coconut coir Mix.*	1.606
Perlite	0.739
Growstone	1.621

* Used in the Growstone mixture.

1.1.4 Phosphorus Adsorption Isotherms

Phosphorus sorption isotherms were measured with the batch technique. Substrates and their mixtures were air-dried and a 1-gram subsample (0.5 g in case of perlite) added to 50 ml equilibration tubes. Then 20 ml (10 ml for perlite) of KH_2PO_4 solution with concentrations of 0, 1, 5, 10, 50, and 100 mg $P.L^{-1}$ in the background of 0.01 M $CaCl_2$ were added to the tubes to obtain a soil/solution ratio of 1:20. The samples were left to equilibrate for 24 hours in an end-over-end shaker. Experiments were conducted in triplicate for each substrate. Tubes were then placed in a centrifuge for 20 minutes at 12000 rpm to physically separate solution from the solid particles. Solutions were then passed through paper filters with 0.2 µm opening size with syringes in order to remove fine particles and get a clean solution for phosphorus concentration measurements.

The analysis of the filtrate soluble reactive phosphorus was carried out with the ascorbic acid colorimetric method. Required reagents were prepared as follows: *Molybdate Reagent*: 12.0 g of ammonium molybdate was dissolved in 250 ml of deionized water and 0.1455 g of antimony potassium tartrate was also dissolved in 500 ml of 5N H_2SO_4. Then 125 ml of ammonium molybdate solution was thoroughly mixed with the 500 ml H_2SO_4/antimony potassium tartrate solution and diluted to one liter with deionized water using a volumetric flask. *Mixed Color Developing Reagent*: in a 1L volumetric flask, 0.739 g of ascorbic acid was dissolved in deionized water then added with 70 ml of the Molybdate Reagent and brought to volume. Since the reliable range of the spectrophotometer's measurement was up to 4 ppm, for higher concentrations we diluted sample solutions with concentrations of 5, 10, 50, and 100 ppm by dilution factors of 2, 4, 20, and 40, respectively. A series of standard PO_4-P solutions in concentrations of 0, 1, 2, 3, and 4 ppm, were prepared for calibration of the spectrophotometer each time a measurement was made. 1 ml of sample solution (diluted sample for higher concentrations) was mixed with 9 ml of color developing reagent in a small tube and its *P* concentration was measured after about 1 hour with a spectrophotometer at 880 nm wavelength.

Because colorimetric determination of the phosphorus concentration requires a clear solution, which was not the case for samples containing considerable amounts of coconut coir (i.e. coconut coir, perlite-coconut coir, Growstone – coconut coir), the total phosphorus concentration for these samples was measured with Inductively Coupled Plasma Mass Spectrometry (ICP-MS) at the Arizona Laboratory for Emerging Contaminants (ALEC).

The linearized Langmuir adsorption equation was fitted to the measured data to obtain each substrate sorption parameters:

$$\frac{C}{S} = \frac{1}{k\,S_{max}} + \frac{C}{S_{max}}$$

where S = S' + S_0, the total amount of *P* retained (mg kg^{-1}) in which S' = P retained by the solid phase (mg kg^{-1}) and S_0 = P originally sorbed onto the solid phase (previously adsorbed *P*), (mg kg^{-1}). C = concentration of *P* after 24 h equilibration (mg L^{-1}), S_{max} = P sorption maximum (mg kg^{-1}), and k = a constant related to the bonding energy, L (mg P)$^{-1}$.

Adsorption data should be corrected for previously adsorbed *P* (S_0) and the least squares fit method is shown to be an acceptable approach (Kovar and Pierzynski, 2009) which is based on the linear relationship between S' and C at low equilibrium *P* concentrations:

$$S' = K'\,C - S_0$$

where K' = the linear adsorption coefficient. We considered the two first lower concentrations (0 and 1 ppm) in this regard to obtain S_0 for each substrate. The calculated Langmuir equation parameters are listed in Table 6.

Table 6. Langmuir P adsorption isotherm parameters

Substrate	S_{max} *(mg.kg^{-1})*	*k (L.mg-1 KH2PO4-P)*
Perlite*	17.95	0.984
Tuff*	270.60	0.066
Coconut coir**	22.98	0.548
Perlite - Coconut coir**	24.15	0.327
Tuff - Coconut coir*	241.82	0.102
Growstone - Coconut coir**	265.49	0.036

* Colorimetric

** ICP-MS

1.1.5 Ammonium Adsorption Isotherms

Ammonium adsorption isotherms where calorimetrically determined in batch experiments similar to the phosphorus isotherms. Ammonium solutions were prepared in 0, 1, 5, 10, 50, and 100 mg NH_4Cl-N.L^{-1}. One gram of each substrate was agitated with 20 ml of the ammonium solutions in a centrifuge tube for 3 hours after adjusting the pH to the range of 6.5 to 7.0 using 1M sodium hydroxide. Samples were then centrifuged and filtered with 0.2 µm filter paper. The concentration of ammonium was measured with the Salicylate method as suggested in Kempers and Zweers (1986) with the following reagents:

1. *Sodiumsalicylate - sodiumnitroprusside*: 33 grams of $NaC_7H_5O_3$ and 20 milligrams of $Na_2Fe(CN)_5NO.5H_2O$ were dissolved in deionized water and diluted to 100 ml.

2. *Buffer*: 9.33 grams of sodiumcitrate.$2H_2O$ and 4.0 grams of NaOH were dissolved in deionized water and diluted to 100 ml.
3. *Hypochlorite*: 5 ml of commercial hypochlorite (10% active chlorine) was dissolved in 25 ml deionized water.

Four ml of extracted ammonium solution in a standard glass tube was mixed with 0.9 ml combined reagent (by mixing 1 part of reagent 1 with 2 parts of reagent 2). Then within one minute 0.1 ml of reagent 3 was added to the tube and then placed in the dark at room temperature for 120 minutes to develop the emerald blue color. The absorbance of the chromophore was measured with a spectrophotometer at 647 nm wavelength. The Langmuir adsorption parameters for ammonium are listed in Table 7.

Table 7. Langmuir adsorption isotherm parameters for ammonium.

	S_{max} $(mg.kg^{-1})$	k $(L.mg^{-1}$ NH_4-$N)$
Perlite	43.6	3.376
Tuff	432.8	0.135
Coconut coir	1419.5	0.036
Perlite - Coconut coir	809.0	0.056
Tuff - Coconut coir	517.3	0.083
Growstone - Coconut coir	473.6	0.054

1.2 Numerical Modeling

We initially developed the numerical model in HYDRUS 2D/3D (*Šimůnek et al., 2012*) to simulate water flow and nutrient transport for the growth system (Fig. 4) used for tomato growth experiments at the Ramat Negev Desert Agro Research Center in Israel.

As a first step, transient moisture distributions in typical greenhouse growth containers were numerically simulated with HYDRUS 3D for different soilless substrates and irrigation management strategies. Each container is populated with 5 tomato plants, each irrigated with a 1.6 l/hr drip emitter. The irrigation water leaving the emitter is split up and supplied via 2 angle arrow drippers located in close vicinity of the plant stems (Fig. 4). The total amount of water supplied to the container per day is 12.5 liter either in 1 single dose (low frequency) or in 18 daily doses (high frequency). The simulation boundary conditions (B.C.) were optimized to match the actual greenhouse growth experiment at the Ramat Negev Desert Agro Research Center. While a variable flux B.C. was applied at locations where water enters the container via the angle arrow drippers, an atmospheric B.C. with an evapotranspirative flux equivalent to 12.5 liter per was established for the remaining top surface. For the 7 drainage openings at the bottom a free drainage B.C. was used. Initially, preliminary literature data (*Chamindu Deepagoda et al., 2012*) were applied for HYDRUS 2D/3D parametrization (Fig. 5).

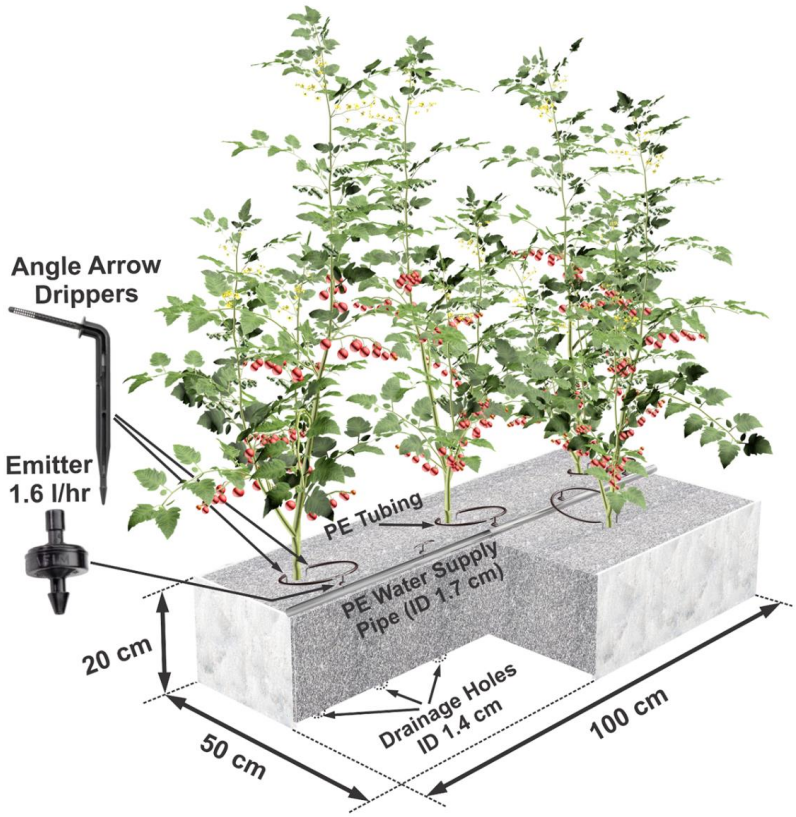

Figure 4: Sketch of a container used for tomato growth experiments at the Ramat Negev Desert Agro Research Center.

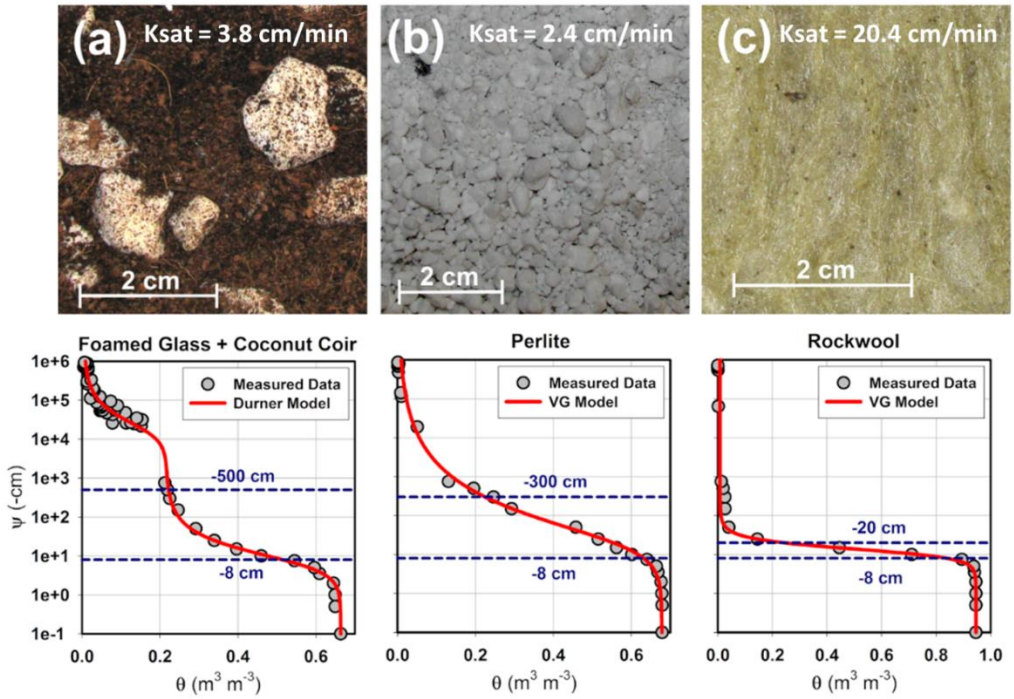

Figure 5: Hydraulic properties of considered soilless substrates (horizontal dashed lines in the soil water characteristic graphs mark the water availability stress limits).

To evaluate substrate performance for low and high frequency irrigation, two criteria were considered; the Critical Window of Diffusivity (CWD) derived from gas diffusivity and porosity (*Chamindu Deepagoda et al., 2012*) to account for aeration, and Water Availability (WA) with stress limits (Fig. 2) defined based on tomato plant physiology (*Thompson et al., 2007*) and irrigation management constraints (*Lieth and Oki, 2008*). Figure 6 depicts snapshots of simulated spatial moisture distributions within the growth substrates short after water application for high-frequency (18 applications per day) irrigation management. Color coding identifies regions that fall within the CDW and WA limits. Visual inspection of Fig. 6 reveals that for these particular snapshots the Growstone® coconut coir mixture seems to perform best, followed by perlite and rockwool.

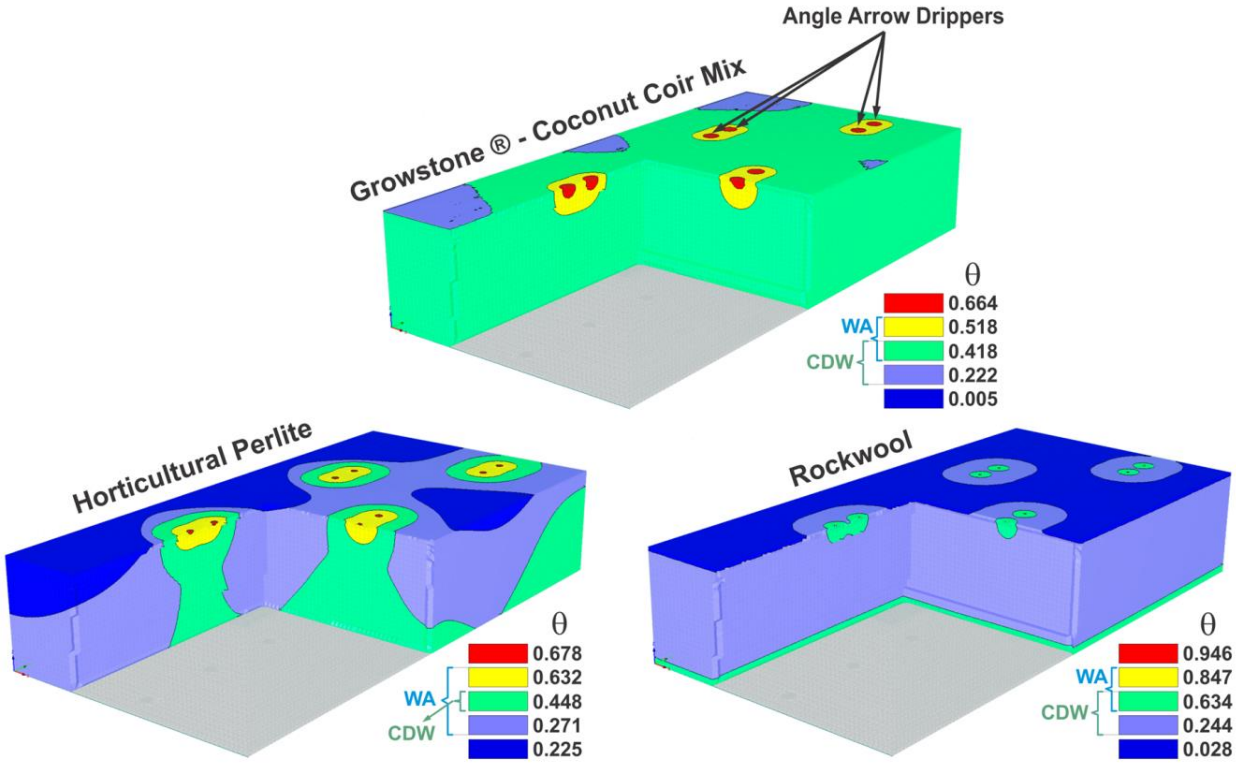

Figure 6: Snapshots of simulated spatial volumetric water content distributions within investigated substrates short after high-frequency water application.

Figure 7 shows the temporal change in substrate/container volume (%) that satisfies both the CDW and WA criteria over several irrigation cycles for low frequency (1 application per day) irrigation management.

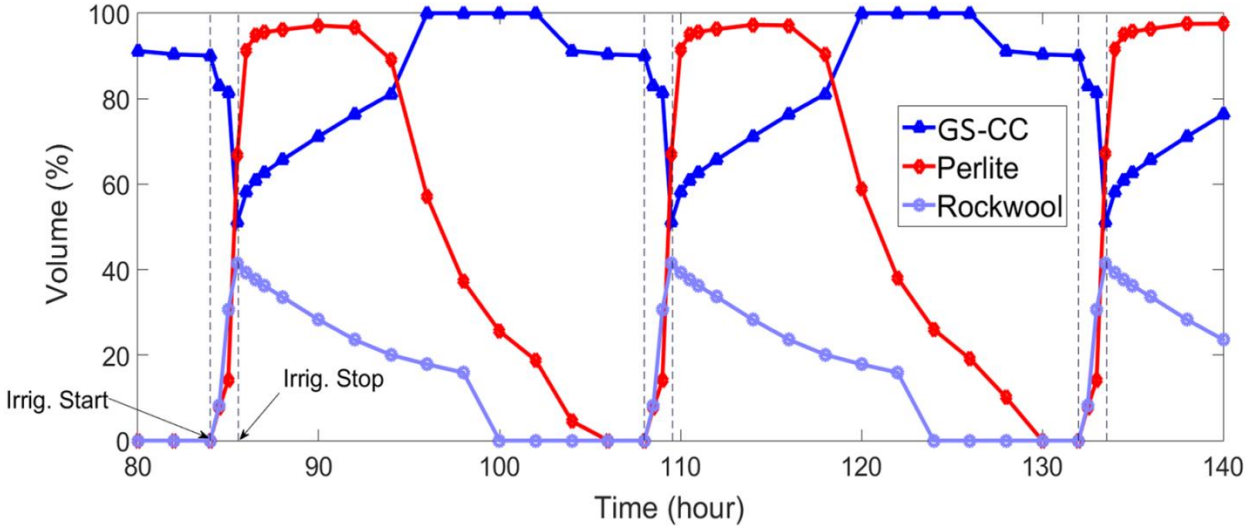

Figure 7: Temporal change in substrate volume (%) that satisfies both the CDW and WA criteria over several cycles of low frequency irrigation.

While a high percentage of the Growstone® coconut coir mixture volume provides seemingly good growth conditions in terms of aeration and water availability, large portions of the perlite and rockwool substrates rapidly desaturate after water application. Most of the rockwool volume never reaches a state that satisfies both the CDW and WA criteria. Obtained simulation results can be potentially used to inform geometrical container design and to optimize irrigation management.

Figure 8 summarizes initial simulation results and compares average substrate volumes (%) satisfying the CWD and WA criteria for low- and high-frequency irrigation. Based on performed simulations it seems that the Growstone® - coconut coir mixture provides a better growth environment than perlite and rockwool. These results may be used to optimize container geometry in concert with irrigation management.

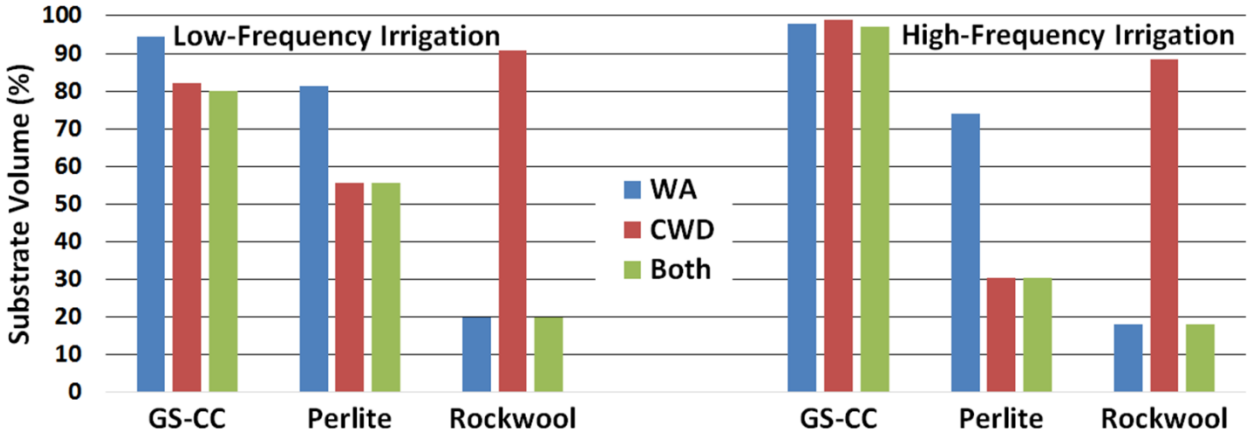

Figure 8: Average substrate volumes (%) satisfying the CWD and WA criteria for low- and high-frequency irrigation.

We also set up the HYDRUS numerical model to simulate non-equilibrium solute transport considering first-order decay reactions to predict NH_4^+, NO_3^-, and H_3PO_4 transport within the growth substrates including NH_4^+ adsorption and transformation to NO_3^-, as well as dissociation of H_3PO_4 to H_2PO_4, HPO_4 and PO_4 to provide feedback for fertigation management.

Simulation results will be applied in conjunction with knowledge gained from growth experiments to "engineer" optimal substrates for specific crops and management strategies by mixing organic and inorganic base materials and modifying relevant parameters such as the particle (aggregate) size distribution.

1.2.1 Nutrient Transport Simulations

We initially invested significant efforts in modeling solute transport with HYDRUS 3D (Šimůnek et al., 2012). Examples for coconut coir and the tuff-coconut coir mixture in a greenhouse growth container (Fig. 9) are presented in the following. Each container was populated with 5 tomato plants, each irrigated with a 1.6 l/hr pressure compensating drip emitter. The total amount of water supplied to the container per day was 5 liters eiter in in 1 or 18 doses.

The evapotranspiration rate was assumed as 5 lit day^{-1} per container and the transpiration rate was calculated to be 0.68 lit day^{-1} with the following equation considering an average Leaf Area Index of 0.3.

$$T_p = ET_p \times [1 - \exp(-0.463 \times LAI)]$$

where TP is the transpiration rate in lit day^{-1}, ETP is the evapotranspiration rate in lit day^{-1}, and LAI is the leaf area index.

Plant root distribution for the early stage of plant development was simulated with a model developed by Vrugt et al. (2001) with parameters set to $z_m = 18\,cm$, $z^* = 3.6\,cm$, $r_m = 13.5\,cm$, $r^* = 0\,cm$, and $p_r = p_z = 1$ (Hanson et al. 2006) as shown in the Fig. 9.

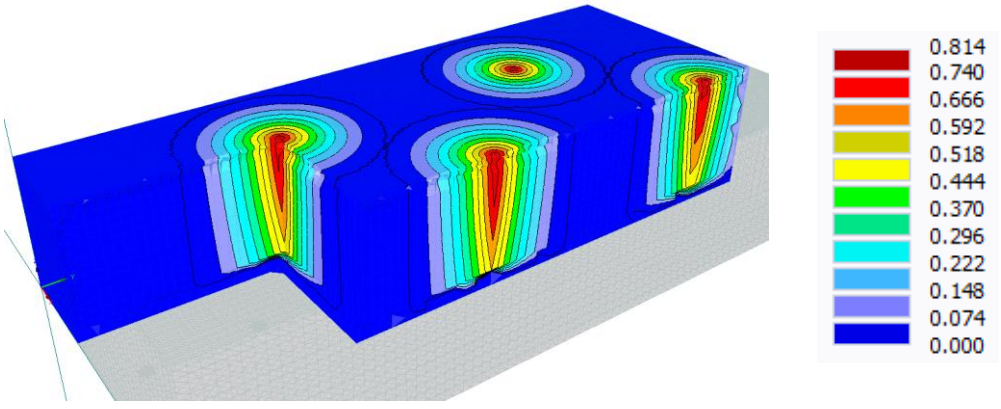

Figure 9: Tomato plant root distribution within the growth container.

The Feddes water stress response function was employed in the simulation with parameters reported in van Dam et al. (1997) adjusting h_{3max} and h_{3min} based on reported soil water content threshold stress values for tomato plants. The applied parameters are listed in Table 8.

Table 8. Feddes water stress response parameters

Feddes parameters	Coconut coir	Tuff - Coconut coir
h_1 [cm]	-1	-1
h_2 [cm]	-2	-2
h_{3max} [cm]	-710	-166
h_{3min} [cm]	-1420	-927
h_4 [cm]	-8000	-8000

For the solute part we considered ammonium (NH_4^+-N), nitrate (NO_3^--N) and phosphorus ($H_2PO_4^-$-P), which are dissolved in the irrigation water at concentrations of 20, 80 and 20 ppm, respectively. Transformation of ammonium to nitrate was considered to be at the rate of 0.2 day^{-1} with a first-order decay reactions model (Hanson et al. 2006). We also simulated the adsorption of ammonium to the solid phase considering a linear adsorption isotherm with a distribution coefficient K_d of 3.5 $cm^3\ g^{-1}$. Phosphorus adsorption to solid phase is simulated by the Langmuir isotherm model with parameters reported in Table 6. It should be noted that nutrient root uptake is considered to be passive, which is the movement of nutrients into the roots by convective mass flow of water, directly coupled with root water uptake.

Figure 10 depicts water balance simulation results for both coconut coir (*C*) and the tuff/coconut coir mixture (*TC*) with low and high irrigation frequencies. While the root water uptake for all four cases are similar, the total water lost because of evaporation and drainage is higher for *TC*. This water loss is about 50% in the case of *C* for both low and high frequency irrigation. It is recognizable that when *TC* is used as substrate, evaporation is higher when applying water at higher rates of irrigation but drainage loss is lower because in this case water is more distributed in the top of substrate profile.

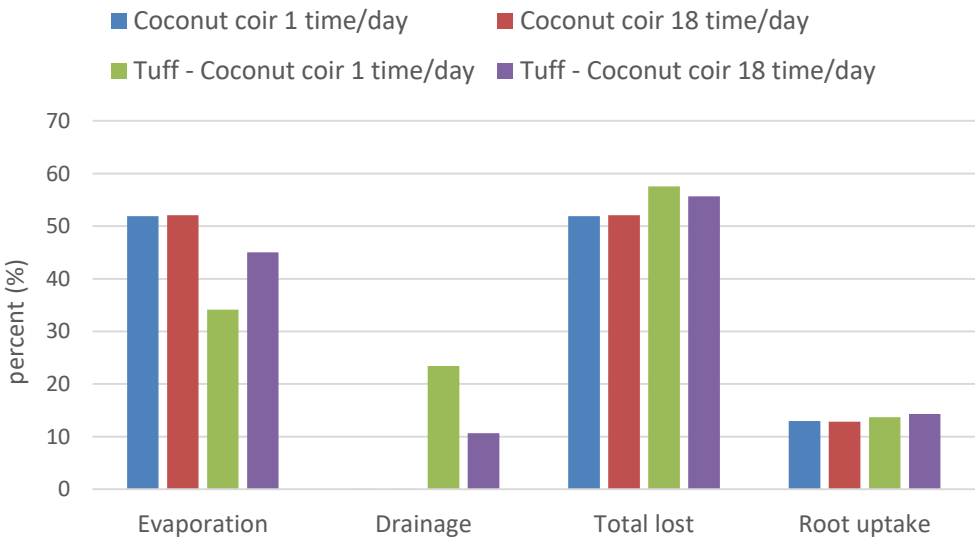

Figure 10: Ratios of evaporation, drainage and root uptake to the irrigated water in percentage

Considering ammonium transport as illustrated in Fig. 11, simulated ammonium uptake by roots is about three times higher for Coconut coir, while the irrigation frequency has no tangible effects. This can be related to the water distribution and the time which roots have access to the dissolved nutrients and also to the amount of nitrified ammonium, which amounted to 62% for coconut coir and 66% for *TC*.

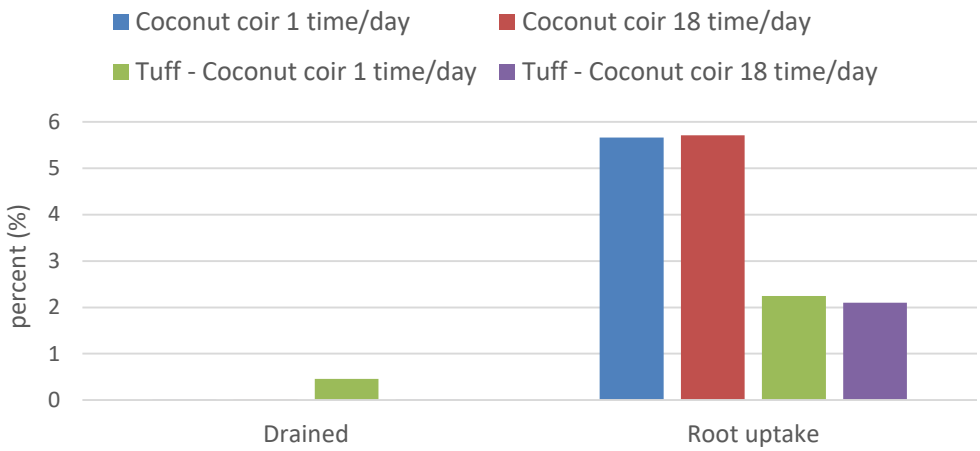

Figure 11: Ratios of drainage and root uptake to the total input ammonium in percentage.

Figure 12 shows the amount of phosphorus uptake by root and also loss due to drainage with the former is almost negligible for the all considered cases. The amount adsorbed by roots is about four times higher when comparing coconut coir and *TC*. This is attributed to the larger capacity of tuff to adsorb and hold phosphorus, corresponding to higher S_{max} value when considering the Langmuir adsorption model that are 59.5 mg kg^{-1} and 4 mg kg^{-1} for tuff and coconut coir, respectively.

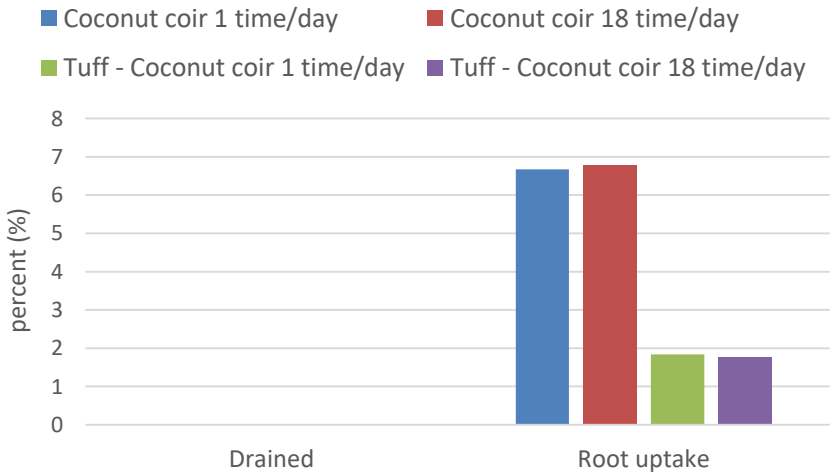

Figure 12: Ratios of drainage and root uptake to the total input phosphorus in percentage.

Results for nitrate transport for the *TC* are not reported here because of issues with numerical convergence encountered when simulating nitrate transport. In the case of Coconut coir for both low and high frequency irrigation 58% of applied nitrate was absorbed by plan roots while the amount of drained nitrate was less than 0.03%. Overall, simulations suggest coconut coir outperforms the tuff-coconut coir mixture with regard to both water balance and water and nutrient (including ammonium and phosphorus) root uptake during the first stage of tomato plants growth. The above simulations should be seen as examples. The simulations will be refined as more data from the greenhouse experiments in Israel become available.

1.3 Adaptation and Modification of the PARSWMS Parallel Code

After we realized that even with a high-powered computer workstation, simulations with HYDRUS 3D (Šimůnek et al., 2012) were not efficient we adapted the Linux-based open source parallel PARSWMS code (Hardelauf et al. 2007). PARSWMS is a parallel version of the SWMS_3D model (Šimůnek et al., 1995), a predecessor of HYDRUS 3D.

Simulation of three-dimensional water flow and solute transport in containerized variably saturated soilless substrates with complex hydraulic properties and boundary conditions necessitates high-resolution discretization of the spatial domain, which commonly leads to several million nodes requiring numerical evaluation. Even today's computational power of workstations is not adequate to tackle such problems within a reasonable timeframe. Hence, parallization of the numerical code and utilization of supercomputers are required. We modified and applied the PARSWMS parallelized code that was developed for Linux and is amenable for solving the 3D Richard's equation for water flow and the convection-dispersion equation for solute transport considering linear solute sorption. The code was modified to allow for nonlinear solute sorption behavior, and applied to simulate water flow and nitrogen and phosphorus transport and transformations in containerized soilless substrates with the University of Arizona "Ocelote" high performance computer cluster. The following scenarios have been simulated to date.

Scenario I

The growth container depicted in Fig. 4, populated with 5 tomato plants, was used as the spatial domain. The considered substrates included perlite, tuff, coconut coir, perlite-coir (50%-50%), and tuff-coir (70%-30%). Each plant is irrigated with a 2 $l.hr^{-1}$ pressure compensating drip emitter. Nitrogen is added to the irrigation system in the forms of ammonium (NH_4^+-N) and nitrate (NO_3^--N) at concentrations of 20 and 80 ppm, respectively, as well as phosphorus at 20 ppm concentration. Adsorption of ammonium and phosphorus to the solid phase is simulated with the nonlinear Langmuir isotherm model with the aforementioned parameters. It should be noted that nutrient root uptake is considered to be passive, which is the movement of nutrients into the roots by convective mass flow of water, directly coupled with root water uptake. Water is supplied either at low (once a day) or high frequency (14 times per day) to meet the plants transpiration demand. To achieve this, the growth season is divided into three growth stages with different root distributions and water requirements. The considered transpiration rates are 5, 12.5, and 20 $l.day^{-1}$ for the first, second and the third stage, respectively, with associated

simulation times of 3, 3, and 2 weeks. The transpiration rate was calculated for each stage from the leaf area index (LAI) as follows:

$$T_p = ET_p \times [1 - \exp(-0.463 \times LAI)]$$

where T_P is the transpiration rate in l.day^{-1}, ET_P is the evapotranspiration rate in l.day^{-1}, and *LAI* is the leaf area index which is considered to be 0.3, 2.5, and 5 for the three stages, respectively (Čereković et al. 2010).

The plant root distribution for the first stage was reproduced based on the model developed by Vrugt et al. (2001) with the parameters: z_m = 17.5 cm, z* = 3.5 cm, r_m = 13 cm, r* = 0 cm, and $p_r = p_z = 1$ (Hanson et al. 2006) as shown in the Fig. 13a. The root distributions for remaining growth stages were mimicked by the water distribution after irrigation applications (Figs. 13b and 13c).

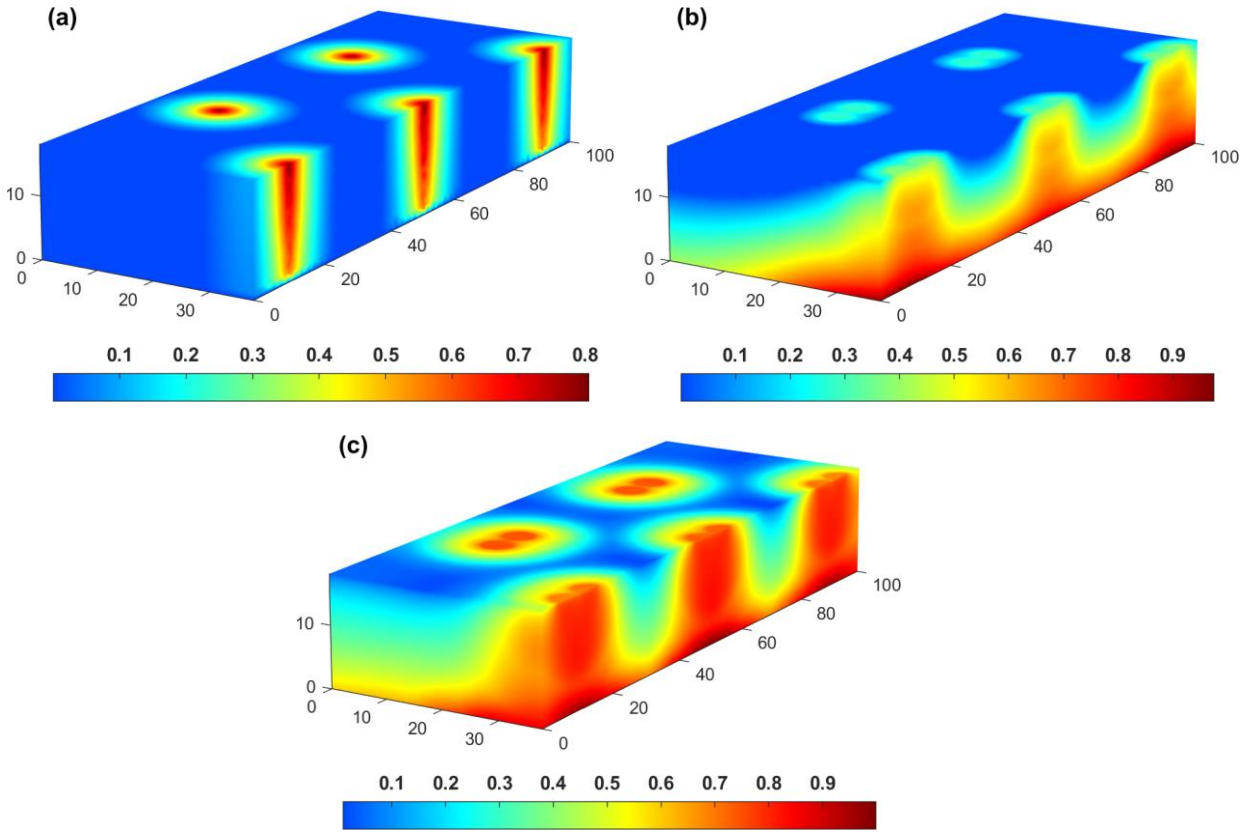

Figure 13: Assumed plant root distributions within the growth containers for the 3 considered growth stages.

The Feddes water stress response function was employed in the simulations with parameters reported in van Dam et al. (1997) while setting the starting pressure head a slightly below the substrates air-entry pressures (Table 9).

Table 9. Feddes water stress response parameters

Substrate	$P0$ (cm)	$POpt$ (cm)	$P2H$ (cm)	$P2L$ (cm)	$P3$ (cm)	$r2H$ (cm.day^{-1})	$r2L$ (cm.day^{-1})
Perlite	-2	-3	-800	-1500	-3000	0.5	0.1
Tuff	-2	-3	-800	-1500	-3000	0.5	0.1
Coconut coir	-23	-24	-800	-1500	-3000	0.5	0.1
Perlite/Coconut coir	-5	-6	-800	-1500	-3000	0.5	0.1
Tuff/Coconut coir	-5	-6	-800	-1500	-3000	0.5	0.1
Growstone/Coconut coir	-1	-2	-800	-1500	-3000	0.5	0.1

Figure 14 depicts the water balance results for all five studied substrates for the two irrigation frequency scenarios (low, with subscript 1, and high, with 14) at the end of the considered growth season (8 weeks). In this figure values for evaporation, root water uptake, and drainage are the percentage of the applied water during this period and the 'satisfied transpiration' is the percentage of potential transpiration that is met by irrigation.

Apart from coconut coir, high irrigation frequency (IF) yielded higher root water uptake and lower water loss due to drainage. The loss due to evaporation is almost the same (except for tuff with low IF). This indicates higher water efficiency for high frequency irrigation.

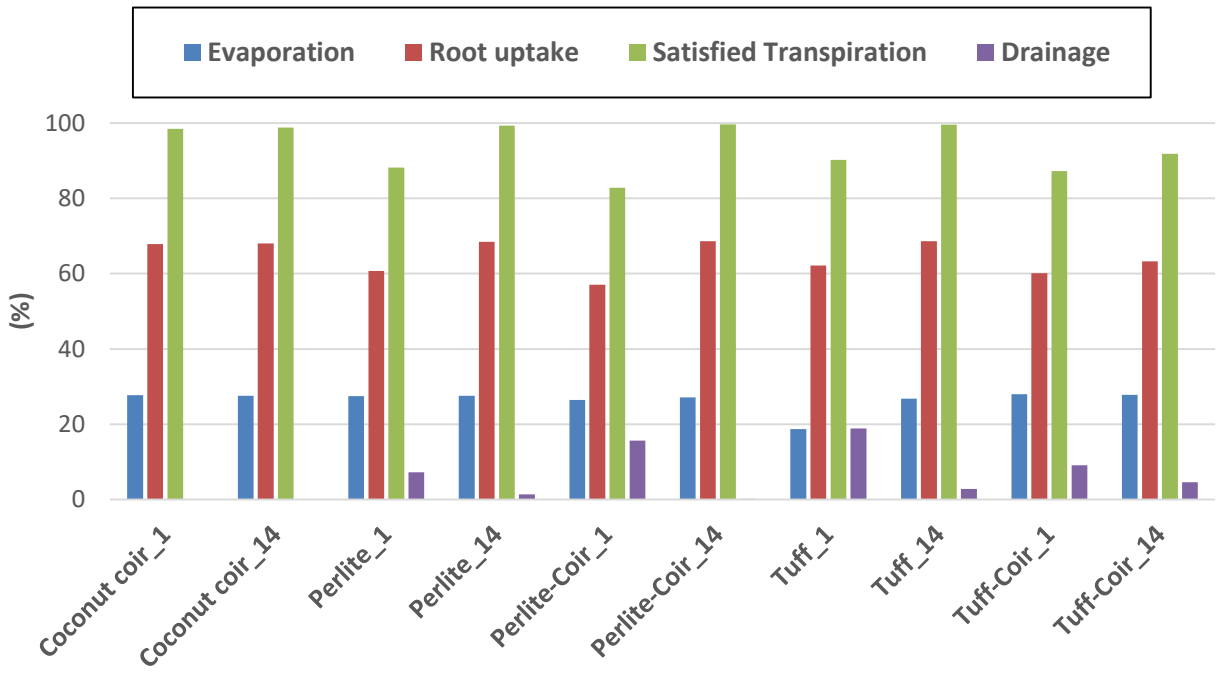

Figure 14: Water balance results for Scenario I simulations.

Results for plant nutrient uptake are depicted in Fig. 15 for each of 3 considered solutes. Here irrigation frequency seems to have no significant influence on the amount of absorbed solutes. For example, in coconut coir more phosphorus than ammonium is adsorbed, which can be attributed to higher capacity of coconut coir to adsorb ammonium than phosphorus. Among different substrates, tuff and tuff-coconut coir showed the lowest amount of ammonium and phosphorus root uptake. This can be explained by the main solute carrying water movement patterns and hence its distribution in the container. This is illustrated in Fig. 16 for two distinct substrates, coconut coir and tuff-coir.

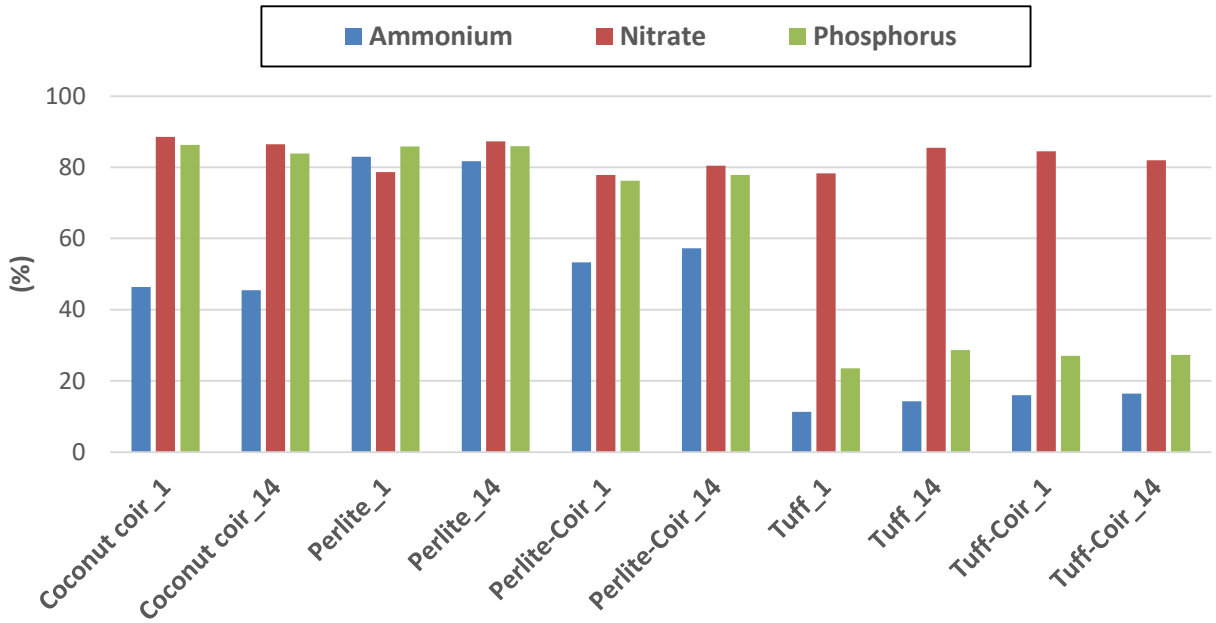

Figure 15: Root nutrient uptake. Values represent percentage of absorbed amount of total applied nutrient.

Figure 16 depicts the water, ammonium, and phosphorus distributions at the end of the last irrigation application, demonstrating different behavior of water in these substrates (more lateral movement in coconut coir when compared to the tuff-coconut coir mixture), which explains the solute distribution difference and hence its availability to the root system. The highest amount of nitrogen and phosphorus loss (because of drainage) is observed in perlite-coconut coir (low IF) followed by tuff (low IF) and perlite (low IF), respectively (results are not shown).

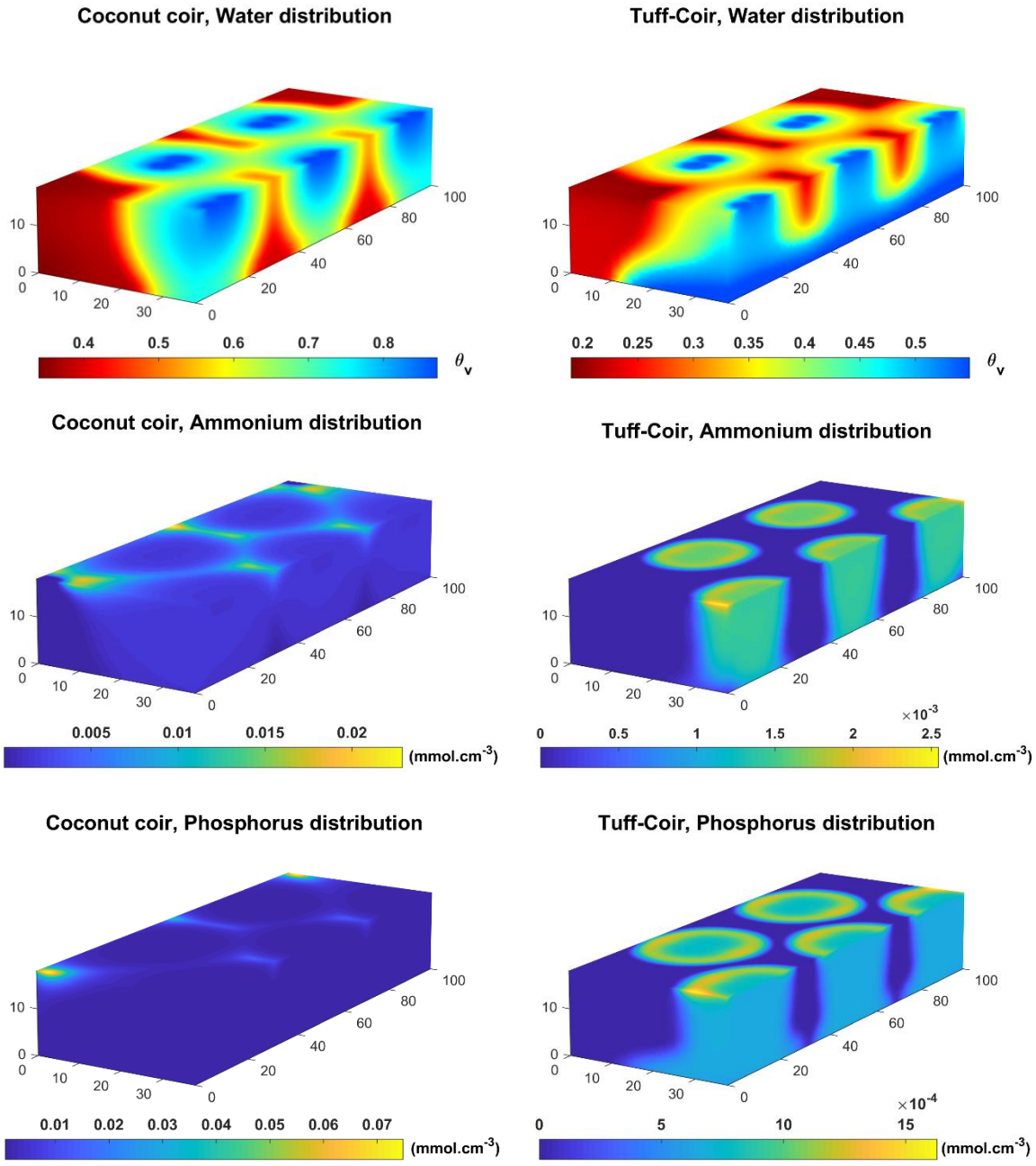

Figure 16: Water, ammonium and phosphorus distributions at the end of simulation for coconut coir (left) and tuff-coconut coir (right) when applying for low frequency irrigation.

Scenarios II and III

Impacts of substrate, water irrigation frequency and container geometry are studied in Scenarios II and III. Selected substrates here are coconut coir, Growstone-coconut coir (50%-50%), tuff, and tuff-coconut coir (70%-30%) with two irrigation frequencies – low (once a day) and high (14 times per day). Two container geometries with about the same volume of 35 l (i.e., 48×50×15 cm and 47×25×30 cm length × width × height) and populated with 3 plants were considered. Water is applied in the same fashion as in Scenario I to meet plant transpiration demands. The same nutrient solutions as in Scenario I were applied (i.e., ammonium, nitrate, and phosphorus with concentrations of 20, 80, and 20 ppm, respectively). Again, the separation of evaporation from transpiration is performed as discussed for Scenario I, for transpiration rates of 3, 7.5, and 12 $l.day^{-1}$ for the three considered plant growth stages and *LAI* values of 0.3, 2.5, and 5.

The Vrugt model parameters for root distribution in the first stage of growth were considered to be: z_m = 14.5 cm, z* = 3 cm, r_m = 11 cm, r* = 0 cm, and $p_r = p_z = 1$. Similar to Scenario I, root development for the second and third growth stages was approximated by spatial water distribution in the containers. Root system distribution for two studied containers and three stages of growth are depicted in Figs. 17 and 18.

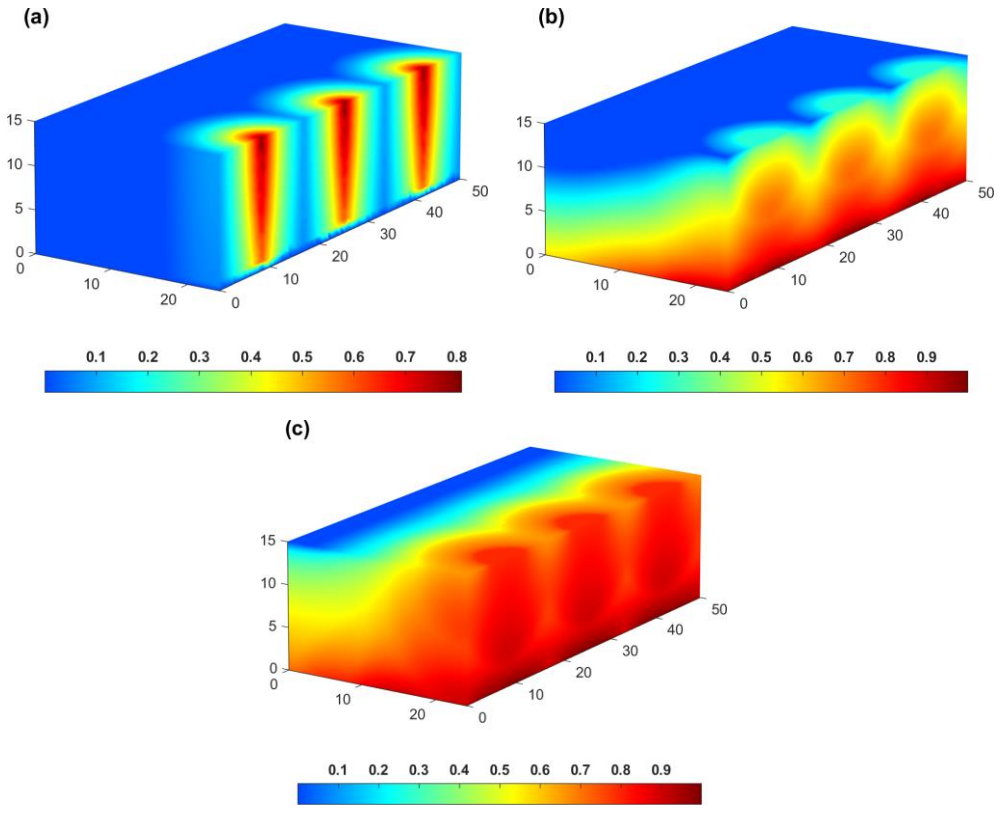

Figure 17: Root distributions for Scenario II for the three considered growth stages.

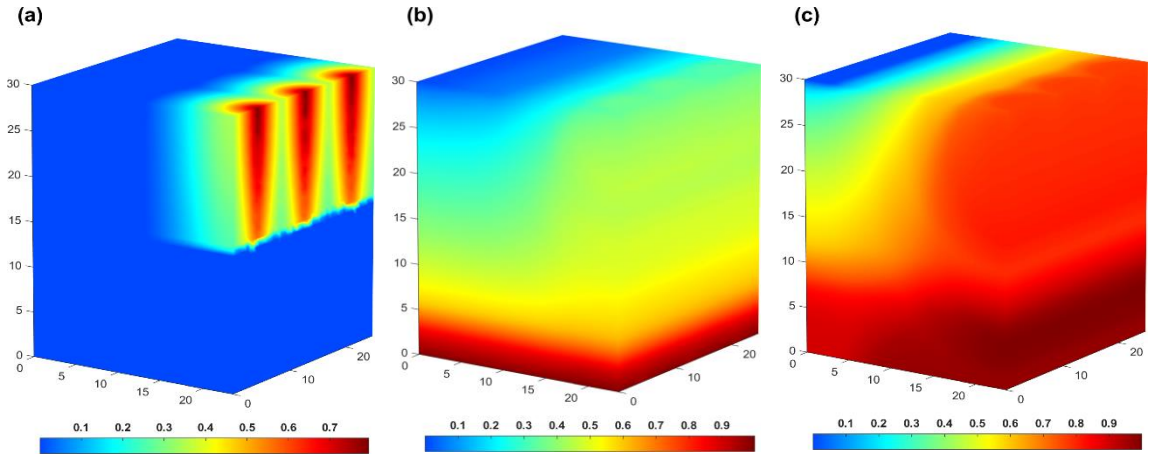

Figure 18: Root distributions for Scenario III for the three considered growth stages.

Water balance information for the two scenarios is depicted in Figs. 19 and 20. In general, less tall containers (Scenario II) outperform taller containers (Scenario III) with regard to water use efficiency. This is more pronounced when applying water at low frequency, where a substantial portion is lost for all considered substrates due to drainage. For high frequency irrigation the performance is almost the same for the two scenarios for tuff and tuff-coconut coir and to some extent for sole coconut coir.

Among all cases of Scenario II, water loss due to drainage was considerable for Growstone-coconut coir (low and high IF irrigation) and tuff (low IF), which yielded lower root water uptake not meeting the plant's transpiration demands. For Scenario III only 3 out of 8 substrate/IF combinations provided more than 80% of the plants' water requirements [i.e., coconut coir (high IF), tuff (high IF), and tuff-coir (high IF)]

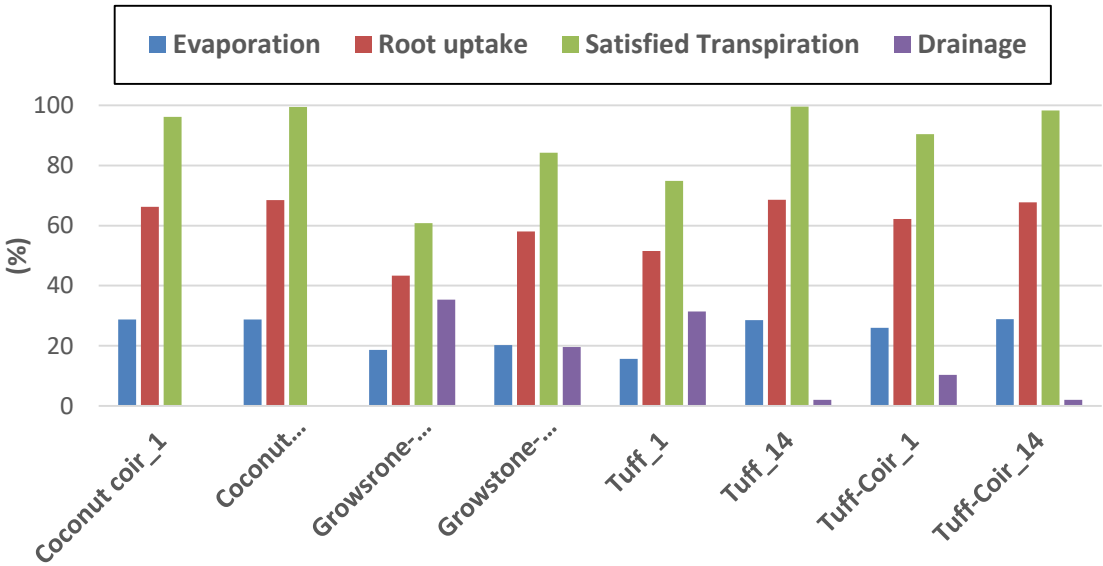

Figure 19: Water balance information for simulations for Scenario II. The satisfied transpiration is calculated from potential transpiration and the remaining water balance components are the percentage of total applied water.

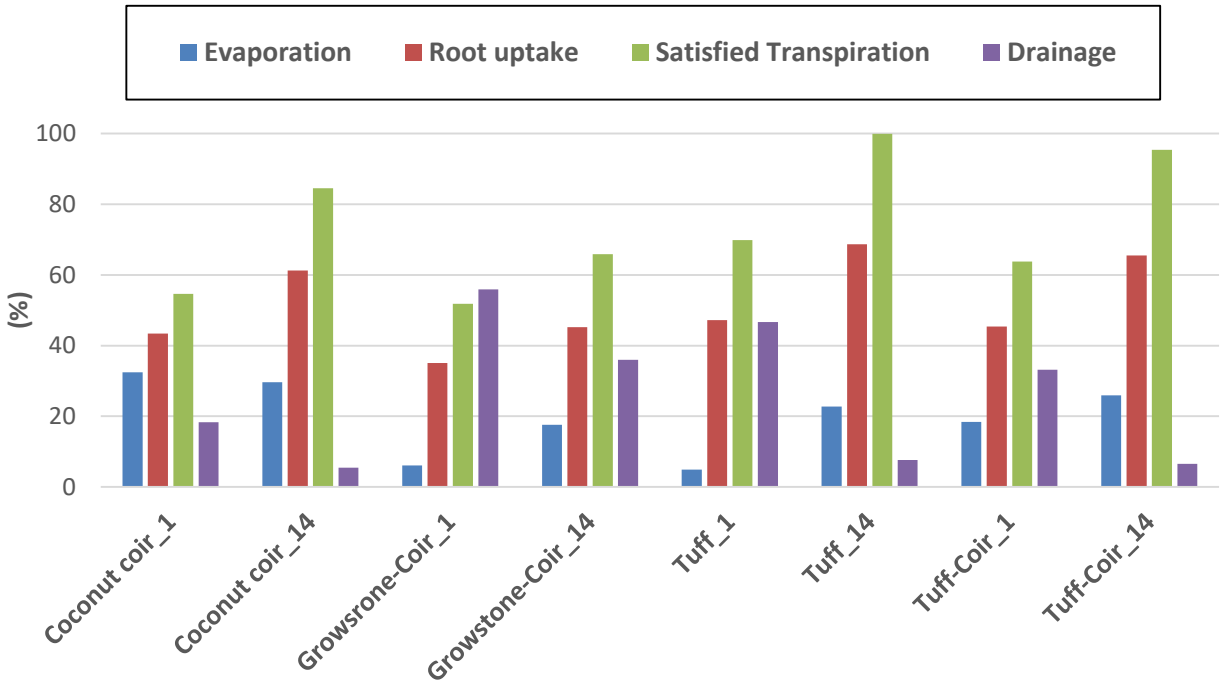

Figure 20: Water balance information for simulations for Scenario III. The satisfied transpiration is calculated from potential transpiration and the remaining water balance components are the percentage of total applied water.

Figure 21 shows the percentages of plant-absorbed ammonium, nitrate, and phosphorus for both Scenario II and III. The highest amount of ammonium absorption took place in coconut coir (low and high IF) in both container geometries and was greater in Scenario II. This was also true in case of phosphorus with absorption rates generally higher for Scenario II for all substrate/IF combinations. Moreover, higher irrigation frequency provided more phosphorus to the plants than low IF. In the case of nitrate, increasing the container height (Scenario III) decreases the amount of supplied nitrogen in most of substrates. Also the highest amount of nitrogen and phosphorus loss (due to drainage) was observed in Growstone-coir (both IFs) and tuff (low IF).

Considering both the water balance and nutrient uptake results, containers with a height of 15 cm are favorable in terms of water efficiency and plant nutrient uptake. Among the substrate/IF combinations the coconut coir and tuff-coconut coir showed the best performance in the less tall container.

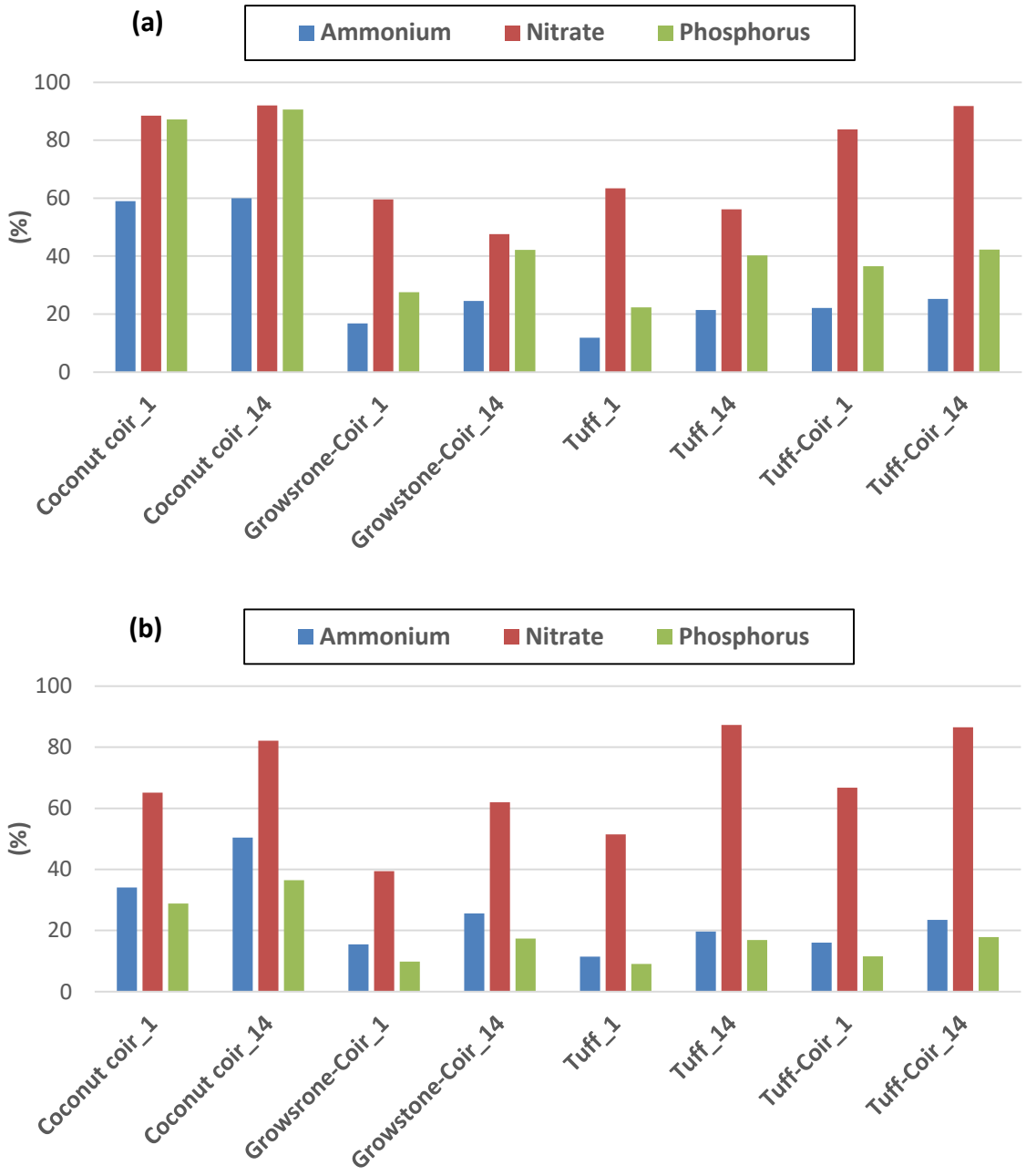

Figure 21: Ammonium, nitrate, and phosphorus plant uptake for Scenario II (a) and Scenario III (b). Values represent percentage of absorbed amount of total applied nutrients.

1.4 Development of a Framework for Estimation of the Water Characteristic of Substrate Mixtures

Individual soilless substrates with desirable and complementing properties for plant development and production are commonly mixed at varying ratios. Organic components, such as coconut coir, often lack coarse particles necessary for adequate aeration and they hold moisture relatively tight in small pores. To optimize aeration and water holding properties they are commonly mixed with coarser materials such as volcanic tuff to create larger pores that rapidly drain after irrigation, thereby creating optimal rhizosphere conditions that can be tailored for a specific crop. Such mixtures often exhibit bimodal pore size distributions and water retention characteristics, where the fraction of smaller pores mainly retains water and the larger pore fraction allows for optimal aeration. The optimum mixing ratios are commonly selected through trial and error by growing plants in a series of mixtures. Replacing this trial and error approach with physical relationships for prediction of mixture behavior from well characterized constituent properties will significantly advance soilless culture production and eliminate costly mistrials. Based on this premise, the SWCs of three mixing ratios of dual component substrates made up of perlite, tuff, and coconut coir have been studied.

Theory

To extend the formalism of statistical mechanics of many-particle systems and to link their microscopic and macroscopic properties, Lu and Torquato (1991, 1992) studied polydisperse particle systems. These are D-dimensional spherical particles of many sizes, which are randomly placed in space. One studied case consisted of impenetrable spheres (Fig. 22).

Figure 22. Schematic of polydisperse impenetrable hard spheres.

To be able to calculate void quantities they defined the void exclusion probability, $e_V(\delta)$, as the "probability of finding a region which is a D-dimensional spherical cavity of radius δ (centered at some arbitrary point), empty of particle material". In other words, $e_V(\delta)$ is the void of size *r* nearest-surface cumulative density function (CDF) in the polydisperse particle system and is approximated as:

$$e_V(\delta) = (1-\eta)\exp[-\pi\rho(c\delta + d\delta^2 + g\delta^3)] \qquad \delta > 0 \tag{1}$$

in which ρ is the number of spheres per unit volume and η, the dimensionless reduced density, *c*, *d*, and *g* are defined as:

$$\eta = \frac{\rho\,\pi^{2/3}\,m_3}{\Gamma\left(\frac{5}{2}\right)} \tag{2}$$

$$c = \frac{4\,m_2}{1-\eta} \tag{3}$$

$$d = \frac{4\,m_1}{1-\eta} + \frac{12\,\xi_2}{(1-\xi_3)^2}\,m_2 \tag{4}$$

$$g = \frac{4}{3(1-\eta)} + \frac{4\,\xi_2}{(1-\eta)^2} + \frac{16}{3}\,\frac{A\,{\xi_2}^2}{(1-\eta)^3}\,m_2 \tag{5}$$

with

$$\xi_k = \frac{\pi}{3}\rho\,2^{k-1}\,m_k \tag{6}$$

Here *A* = 2 is the Carnaham-Starling approximation and m_k is the *k*-th moment of the probability density function (PDF), *f(R)*, for the sphere sizes, *R*:

$$m_k = \int_0^\infty R^k\,f(R)\,dR \tag{7}$$

The CDF of the pore-size distribution is then determined as:

$$P(\delta) = 1 - \frac{e_V(\delta)}{\phi} \tag{8}$$

where ϕ is the porosity. Since the definition of the pores by Lu and Torquato is not the usual definition of pores determined with porosimetry technics and is biased toward smaller values, Chan and Govindaraju (2004) proposed the effective pore-size value, r_p, linearly related to pore-size defined by Lu and Torquato, δ, as: $r_p = \alpha\,\delta$ and assumed as lognormal distribution of the particle sizes. They successfully applied their model to sand and loamy sand soils but failed for other textures.

As Chan and Govindaraju (2004) stated, assuming a linear relationship between δ and r_p is a potential limitation of their model. We propose a power relationship, which adds great flexibility to the model that relates particle size distribution (PSD) to the soil water characteristic curve. The new proposed relationship is:

$$\delta = a\,{r_p}^b \tag{9}$$

in which *a* and *b* are fitting parameters. Effective pore-size PDF, $p_e(r_p)$, is related to the effective soil water saturation, Θ, as (Kosugi, 1994; Chan and Govindaraju, 2003):

$$p_e(r_p) = \frac{d\Theta}{dr_p} \tag{10}$$

where

$$\Theta = \frac{\theta - \theta_r}{\theta_s - \theta_r} \tag{11}$$

Integrating Eq. 10 and employing Eq. 8 and 9 yields:

$$\Theta(r_p) = \int_0^{r_p} p_e(\zeta)\, d\zeta = 1 - \frac{e_V(a\, {r_p}^b)}{\phi} \tag{12}$$

By relating the pore radius to the capillary pressure head, *h*, using the Young-Laplace equation we receive:

$$h = \frac{2\,\sigma\, cos(\psi)}{\rho\, g} \cdot \frac{1}{r_p} = \frac{c_0}{r_p} \tag{13}$$

where σ is the interfacial tension between air and water, ψ the contact angel, ρ the density of water, and *g* is the acceleration due to gravity. c_0 at the room temperature and for the contact angel of zero is equal to 0.149 cm^2. The final equation relating the capillary pressure and soil water content is then:

$$\theta(h) = \left\{1 - \frac{e_V\left[a\left(\frac{c_0}{h}\right)^b\right]}{\phi}\right\} \cdot (\theta_s - \theta_r) + \theta_r \tag{14}$$

It should be mentioned that the soil particle (sphere) size distribution, *f(R)*, could be of any form and here for the sake of flexibility it is assumed as a Weibull distribution:

$$f(R, \alpha, \beta) = \frac{\beta}{\alpha}\left(\frac{R}{\alpha}\right)^{\beta-1} \exp\left[-\left(\frac{R}{\alpha}\right)^{\beta}\right] \qquad R \geq 0 \tag{15}$$

Hence, the *k*-th moment of the distribution in Eq. 7, is calculated as:

$$m_k = \alpha^k\, \Gamma\left(1 + \frac{k}{\beta}\right) \tag{16}$$

Model Application

The main idea of predicting the SWC of the mixture from known SWCs of the individual constituents is to derive the PSDs of them and then calculate the PSD of the mixture. Then the SWC of the mixture can be approximated by its PSD. The translation between SWC and PSD is carried out by the new proposed model. At this stage, since we do not have a priori knowledge about the range of two fitting parameters in Eq. 9 for each soil texture, the obtained PSD from fitting Eq. 14 to the SWC curve is not the actual PSD and because of this I we denote it as pseudo-PSD. Note that the model works well when PSD data are available.

As the first step Eq. 14 is fitted to the SWC curves of our three constituent substrates, perlite, tuff, and coconut coir to find the best values for *a*, *b*, α, and β. Fig. 23 shows the measured data points of θ-*h* pairs and fitted Eq. 14 for the three constituent substrates.

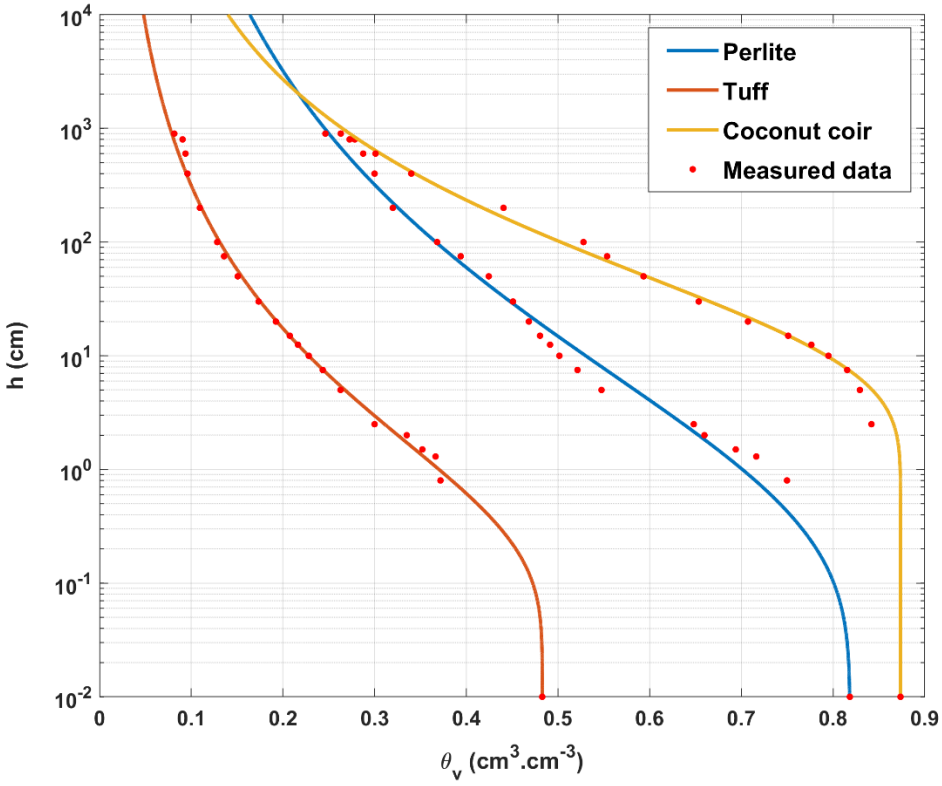

Figure 23. Water characteristic curves for the Perlite, Tuff, and Coconut coir from measured data and Eq. 14.

Derived values for the four parameters of each substrate are listed in Table 10 and Figures 24 and 25 depict their plots.

Table 10. Model parameters for the three considered individual constituent substrates.

Substrate	*a*	*b*	*α*	β
Perlite	1.427	0.149	2.119	1.192
Tuff	0.458	0.262	6.944	1.382
Coconut coir	1.031	0.228	1.414	1.386

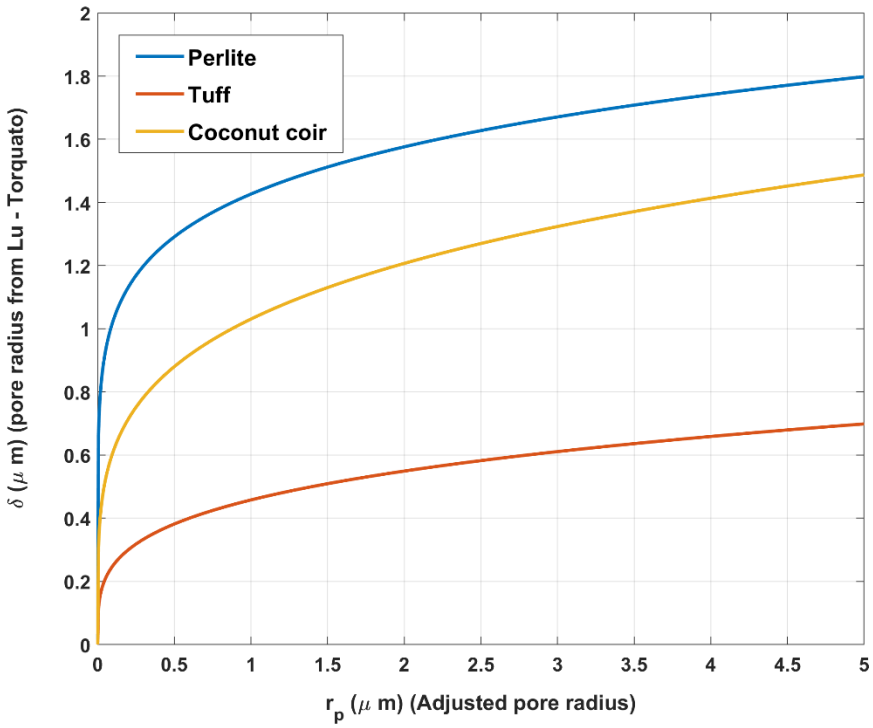

Figure 24. Plots of Eq. 9 for the three considered constituent substrates.

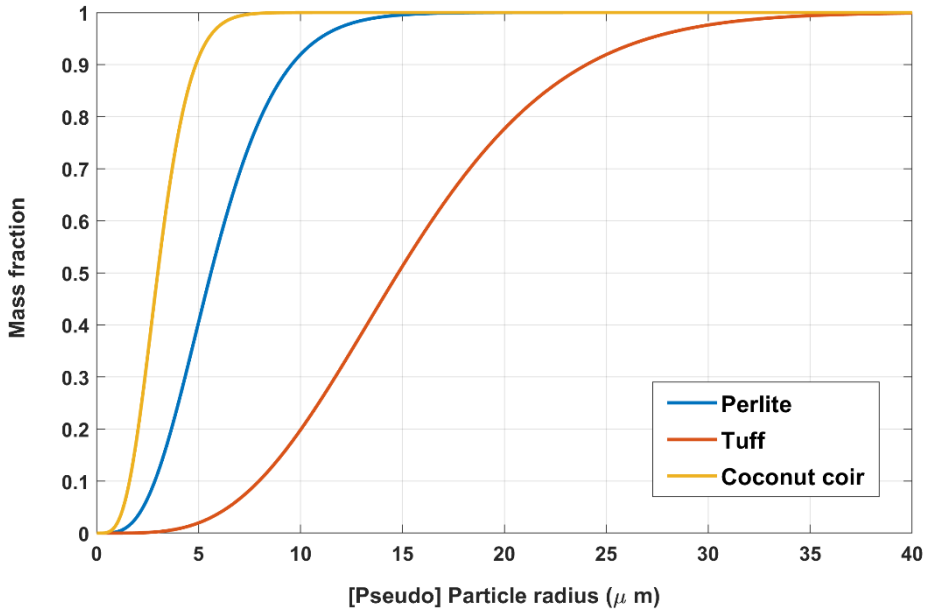

Figure 25. Pseudo cumulative particle radius distribution for the three considered constituent substrates.

It should be noted that since the PSD in Lu-Torquato is expressed as the number of spheres with the particular radius, *R*, and the PSD in the soil science is usually expressed as the mass fraction, *M*(*R*), values in Fig. 25 are calculated as:

$$M(R) = \left\{\int_0^R \zeta^3 f(\zeta,\alpha,\beta)\, d\zeta\right\}/m_3 \qquad (17)$$

Eq. 17 is solved numerically in order to plot Fig. 25. The next step considers the weighted sum of two constituent PSDs, C_1 and C_2, with the volumetric ratio of *w* calculated:

$$f(R) = w\, f(R,\alpha_1,\beta_1) + (1-w)\, f(R,\alpha_2,\beta_2) \qquad (18)$$

and a Weibull distribution is fitted to it in order to derive mixture's PSD parameters α_{mix} and β_{mix}. The other required parameters of mixture's SWC curve are then a_{mix}, b_{mix}, $\theta_{s\ mix}$, and $\theta_{r\ mix}$. In the case of two latter parameters the weighted harmonic mean of corresponding constituents' parameters is employed and as could be observed in Fig. 26 and 27 is a reasonable estimate. For a_{mix} and b_{mix} we investigated different averaging schemes and the following two yielded the best results. For the perlite-coconut coir mixtures for which their constituents' SWC curves intercept (as could be seen in Fig. 26), a_{mix} and b_{mix} is obtained by fitting a power function of the form $a_{mix} {r_p}^{b_{mix}}$ to the following weighted sum equation:

$$\delta_{mix} = w\, a_1 {r_p}^{b_1} + (1-w)\, a_2\, {r_p}^{b_2} \qquad (19)$$

For the tuff-coconut coir mixtures (with no interception of corresponding constituents' SWC curves), a_{mix} is the weighted arithmetic mean and b_{mix} is the weighted geometric mean of corresponding parameters of the two constituents. Predicted SWC curves of the mixtures are shown in Fig. 26 and 27 for perlite-coconut coir and tuff-coconut coir mixtures, respectively.

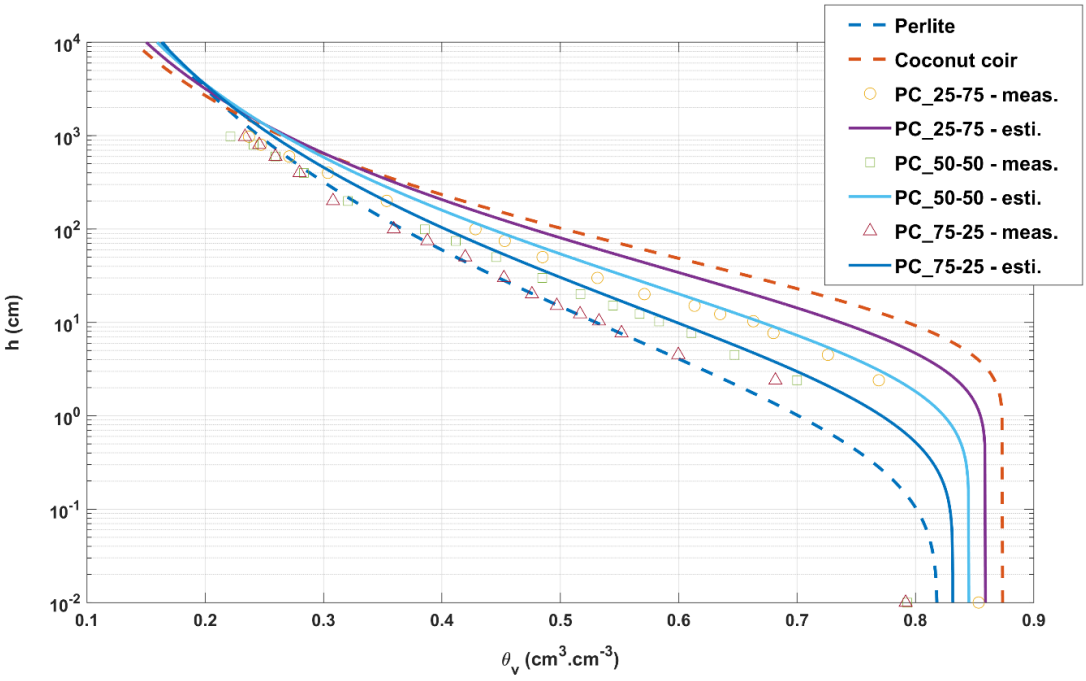

Figure 26. Estimated SWC curves of the mixtures of perlite and coconut coir using the new model.

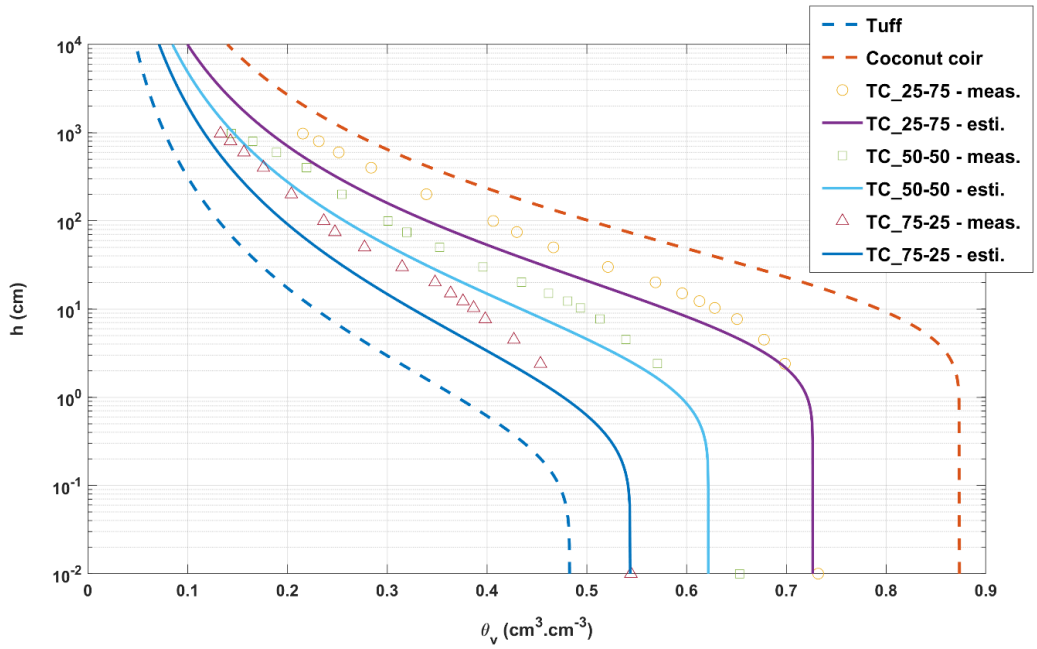

Figure 27. Estimated SWC curves of the mixtures of tuff and coconut coir using the new model.

2. Achievements - ARO Volcani Center

2.1 Greenhouse Experiments

Experiment I: August 2015 - May 2016

The first year greenhouse experiment was conducted at the Ramat Negev Experimental Station between August 24, 2015 and May 8, 2016 (Fig. 28). Tomatoes were grown in 100×50×18 (Length, Width, Height) containers with five soilless media that included tuff, perlite, coconut coir, a tuff/coconut coir mixture (70/30 vol.-%), and a perlite/coconut coir mixture (50/50 vol.-%). Each container was either irrigated with high frequency (11-14 pulses per day depending on the applied amount of water) or with low irrigation frequency (1 pulse per day). A total of 10 treatments (Fig. 29) arranged in 4 blocks were investigated. The tomato transplants were planted in 2 rows on August 24. The distance between plants was within the rows was 40-cm; the distance between rows was 25-cm; and the distance from the rows to the rim of the containers was 12.5-cm. Each container was irrigated with one dripper line in the center of the container, parallel to the rows. The irrigation system consisted of 2 l/h on line emitters, each split into two angle arrow drippers positioned on two sides of each plant as depicted in Fig. 4. On February 2, 2016 the lines were changed to integral drippers of 1.6 l/h, 20-cm between drippers (one dripper for each plant), in the center of the containers. At the same time the greenhouse was covered with a black net providing 50% shading. Each plot was composed of three containers in a row. Drainage was collected from containers highlighted in purple (Fig. 29) and the amount of water was measured and chemical analysis of drainage water was performed. The amount of irrigation during the season was adjusted according to weather conditions and plant water demand.

Figure 28. Tomato growth experiment with different base substrates at the Ramat Negev Experimental Station (August 24, 2015 to May 8, 2016).

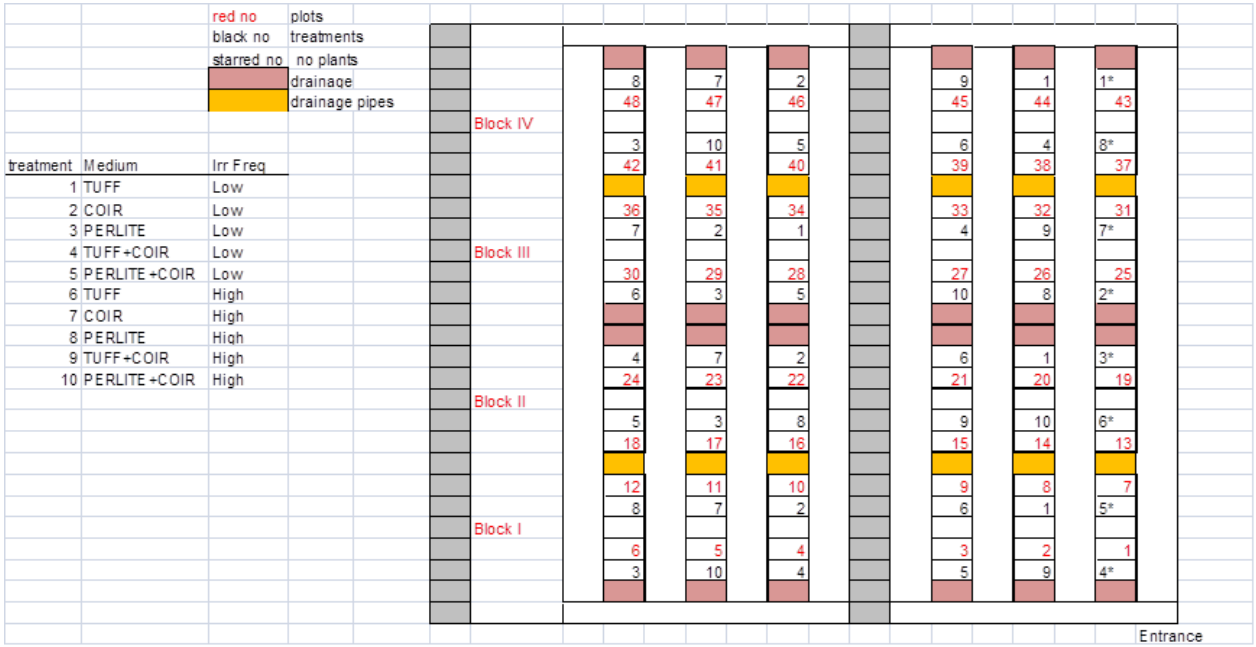

Figure 29. Setup of the tomato growth experiment. Note that the tuff/coconut coir mixture was 70/30 vol.-%, and the perlite/coconut coir mixture 50/50 vol.-%.

Air temperature and humidity in the greenhouse were monitored and recorded continuously throughout the experiment (Fig. 30). Acclima sensors were installed in six of the treatments (1, 2, 3, 6, 7, 8), three substrates (Tuff, Perlite and Coir) combined with the two irrigation frequencies (High and Low), at 5 and 15 cm depths. The sensors were connected to a

datalogger that recorded volumetric water contents, temperatures and bulk electrical conductivity (EC) in 5 min intervals.

The tomato yield was recorded throughout the entire season by selective harvesting of ripe fruits from the central container of each plot, 1 to 3 times per week according to the ripening rate. The fruits were classified to quality standards and monitoring of physiological disorders. Leave samples were taken on November 24, 2015. Whole plant samples were collected on December 31, 2015, on March 23, 2016, and at the termination of the experiment on May 8, 2016 (one plant per plot on the first two sampling dates and 3 plants at termination). Plant organs were dried at 65oC), fresh and dry weight were determined and subsamples were ground and digested with sulfuric acid for essential nutrient (N, P, K) analyses.

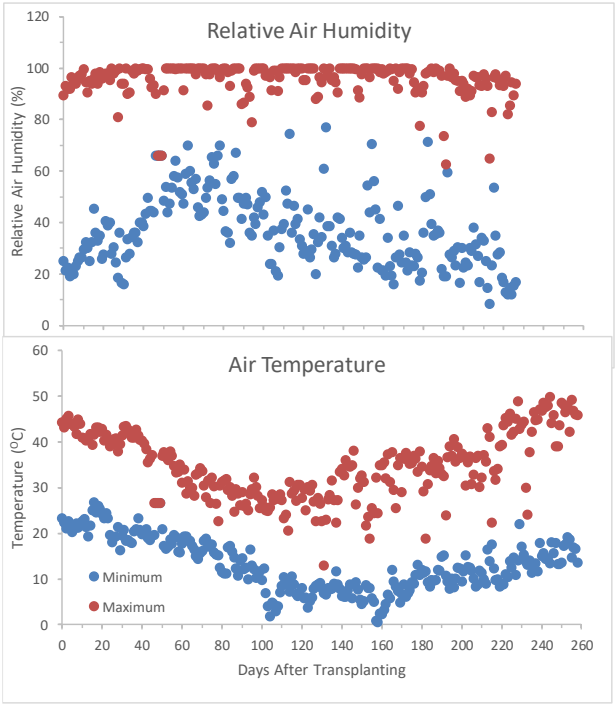

Figure 30: Daily maximum and minimum values of air temperature and humidity during tomato growth in the greenhouse at the Ramat Negev Experiment Station (August 24, 2015 to May 8, 2016).

The maximum air temperature in the greenhouse at transplanting was about 45°C and in the first 90 days it decreased gradually to a range of 25 to 30°C (90 to 180 days), followed by gradual increase up to 49°C in the 240 to 260 days of tomato growth. The minimum temperature during the first week after transplanting was 20°C, it decreased to 2-12°C during the period of 100 to 160 days after transplanting, and increased to 13-22°C during the last month of the experiment. Thus, the minimum air temperature was about 20 to 30 degrees lower than the maximum with the highest difference during the last month of the experiment. The maximum relative humidity (RH) was within the range of 80 to 100 % throughout the experiment with an average above 90%. These high humidity values were always obtained during night time. Whereas the minimum relative air humidity values were about 20% at

transplanting, increased in the first 60 days to a high range of 45-70% and from day 85 decreased slowly to a wide range of 0-40%.

Water contents and temperatures in the growth media at 5 and 15 cm depth are shown for the period of main tomato fruits harvesting from February 2, 2016 to May 8, 2016 (Fig. 31). In all three measured substrates the moisture at the bottom of the container (15 cm bellow surface) was always higher than in the top layer (5 cm bellow surface), as expected. Higher irrigation frequency reduced the amplitude of water content in all measured substrates at the two positions relative to the low irrigation frequency in agreement with the literature (Heller et al., 2015; Silber et al. 2003, 2005; Xu et al. 2004). The highest moisture content was obtained in the coconut coir substrate, followed by perlite and the lowest in tuff. The higher water content gradient between 5 to 15 cm bellow the container top surface was obtained in coconut coir, followed by perlite and then tuff. No significant effects of irrigation frequency and measured depth on the temperatures were observed (Fig. 32). In all treatments (substrates and irrigation frequencies) there was a daily amplitude of 5 to 10 degrees and the temperature increased gradually from February to May, parallel to the increase in air temperature (from day 180 and on, Fig. 32). In the perlite substrate the daily temperatures amplitude and the increase in temperature from February to May were smaller than in the other substrates, thus the range of temperatures in February in all treatments was 10-15^{o}C, whereas in the last month before experiment terminating the average temperature was 20+5 and 23+7^{o}C in the Perlite and the other substrates, respectively.

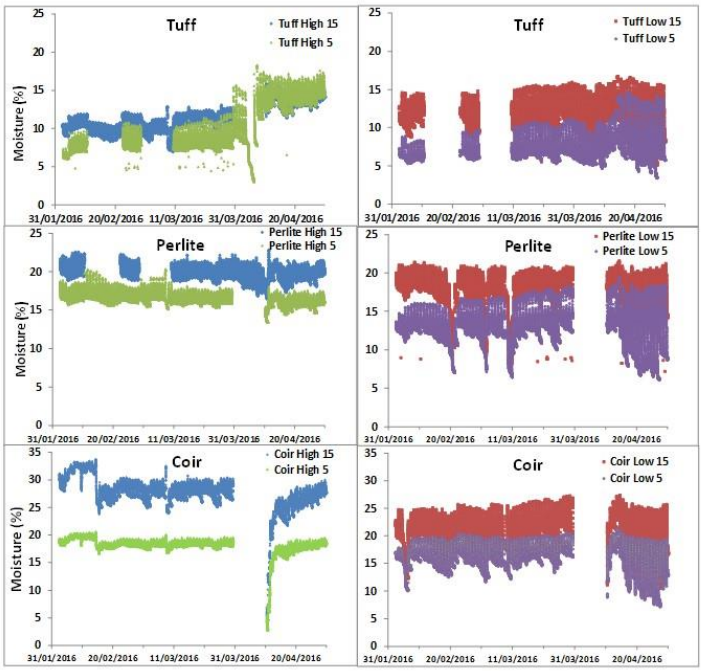

Figure 31: Water content in the growing medium at 5 and 15 cm below the containers surface during tomato growth in the greenhouse at the Ramat Negev Experiment Station (August 24, 2015 to May 8, 2016).

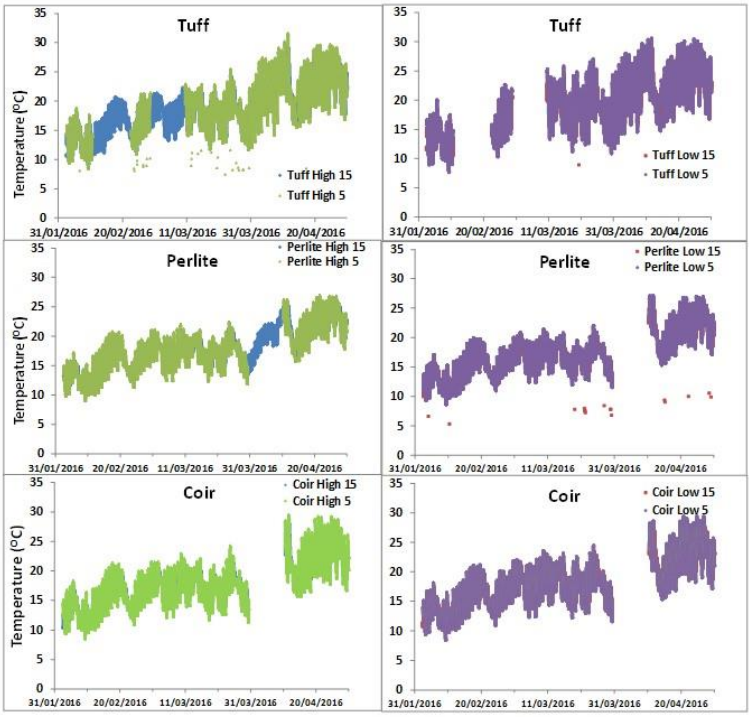

Figure 32: Temperature in the growing medium at 5 and 15 cm below the containers surface during tomato growth in the greenhouse at the Ramat Negev Experiment Station (August 24, 2015 to May 8, 2016).

High irrigation frequency enhanced the annual fruit yield and the high quality fruit yield significantly, independently of substrate type (Table 11), although the main effects were obtained in the mixture of tuff with coir and in the coir substrates. The type of substrate had significant effect on the high quality fruit yield and on deformed fruits, with the highest high quality yield in the tuff and the lowest in the mixture of Perlite with Coir, and in the other substrates the values were not significantly different from these two extremes. The largest effect of the irrigation frequency was obtained in the Coir; the lowest and highest accumulated fruit yields were obtained in the low and high irrigation frequency in Coir substrate, respectively. Stronger impact of irrigation frequency and substrate type were obtained with the mixtures, where the lowest and highest fruit yields were obtained in the low and high irrigation frequency in the Tuff/Coir mixture, respectively (Table 11). Fruit mean weight was smaller in the low irrigation frequency in the Tuff/Coir and Perlite and Coir substrates, as could be expected, however the opposite effect was obtained in the Perlite/Coir treatment, indicate that in this substrate the number of fruits was reduced by the low irrigation frequency whereas the total weight of the yield was unaffected. The fruit yield as function of time is presented in Fig. 33. The effect of irrigation frequency that was obtained in the Tuff/Coir mixture started 3 months after transplanting and the gap increased with time. In the Coir the effect of irrigation frequency was smaller and started 4 months after transplanting.

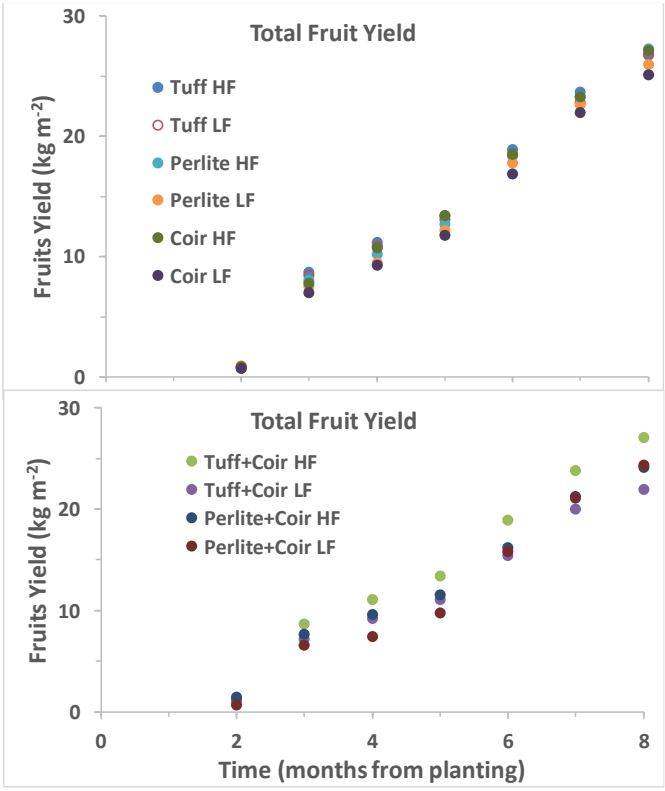

Figure 33: Total fruit yields as a function of time as affected by substrate type and irrigation frequency.

Table 11. Total fruit yield and quality parameters as affected by substrate type and irrigation frequency.

Substrate	Irrigation frequency	Total yield	High quality Yield	BER	Others	Fruit weight
		kg m^{-2}	kg m^{-2}	kg m^{-2}	kg m^{-2}	g/fruit
Tuff	High	26.8	24.4	0.91	1.41	121.3
Tuff	Low	26.8	24.1	1.13	1.55	119.1
Tuff/Coir	High	27.1	24.3	1.00	1.77	127.0
Tuff/Coir	Low	22.0	18.8	0.85	2.14	114.1
Perlite	High	27.3	24.4	1.57	1.25	128.9
Perlite	Low	26.0	23.2	1.46	1.32	120.9
Perlite/Coir	High	24.1	21.6	1.10	1.29	121.1
Perlite/Coir	Low	24.3	21.0	1.48	1.61	127.8
Coir	High	27.1	23.9	1.76	1.42	125.4
Coir	Low	25.1	22.5	1.33	1.25	121.1
Variable	df			Prob > F		
Substrate	4	0.0859	0.0317*	0.0833	0.0024*	-
Irrigation	1	0.0115*	0.0186*	0.3201	0.5324	-
Block	3	0.4406	0.3817	0.6052	0.0650	-
Substr. *Irr.	4	0.1852	0.1994	0.8244	0.5252	-

Significant reduction of stem biomass by low irrigation frequency over all substrates treatments was obtained in March 2016 (Table 12). Substrates and irrigation frequencies had strong impact on plants biomass and the potential yield (fruits that remained on plants after the last selective harvest on April 30th 2016) at termination of the experiment on May 8th, 2016. Stem biomass was significantly reduced by low irrigation frequency in the Tuff and the Tuff/Coir mixture; in the low irrigation frequency the stem biomass was significantly lower in the Tuff and the Tuff/Coir mixture than the other substrate, whereas in the high irrigation frequency lower stem weight was obtained just the Tuff substrate. There was significant interaction effect of irrigation frequency and substrate on fruits weight, thus low irrigation frequency caused a considerable reduction in Tuff/Coir mixture, whereas higher fruit weights were obtained in the low irrigation frequency in the Tuff and the Perlite/Coir mixture.

Table 12. Plants biomass and fruit weight as affected by substrate type and irrigation frequency in March 2016 and at termination of growth on May 8, 2016.

Substrate	Irrigation frequency	December 2015		March 2016		May 2016		
		Stem	Leaves	Stem	Leaves	Stem	Leaves	Fruits
					g/plant			
Tuff	High	540	620	720	270	1070	934	274
Tuff	Low	550	600	700	210	927	753	408
Tuff+Coir	High	790	830	1030	280	1185	892	305
Tuff+Coir	Low	650	610	710	230	938	691	80
Perlite	High	770	760	790	200	1218	854	318
Perlite	Low	640	710	730	280	1233	941	307
Perlite+Coir	High	570	640	900	300	1172	885	325
Perlite+Coir	Low	800	750	660	250	1258	973	468
Coir	High	770	710	1110	280	1228	649	283
Coir	Low	660	710	790	300	1199	882	310
Variable	df				Prob > F			
substrate	4	0.097	0.698	0.1129	0.5360	0.0002*	0.0868	0.0065*
irrigation	1	0.505	0.539	0.0046*	0.5440	0.0245*	0.8927	0.6319
block	3	0.908	0.737	0.7202	0.6922	0.8587	0.7232	0.1096
substrate *Irrigation	4	0.074	0.528	0.3005	0.2674	0.0082*	0.0136*	0.0067*
substrate *block	12	0.782	0.815	0.7547	0.5091	0.2033	0.8399	0.0179*
Irrigation * block	3	0.273	0.892	0.7372	0.4884	0.7093	0.5848	0.4973

The treatments, irrigation frequency and substrate types didn't have significant effect on nitrogen (N) and phosphorus (P) concentrations in plants organs, except the significant effect of the substrate type on roots N concentration (Table 13). Lowest value of root N were obtained in Tuff/Coir mixture (9.2) and highest value in Perlite (16.9) vs 13.9, 14.0 and 14.6 in Coir, perlite/coir mixture and Tuff. High frequency supply of N and P through fertigation in soilless

culture eliminates nutrients' deficiencies, especially nitrogen (Silber and Bar-Tal, 2008). The current results of N concentrations in the tomato plant organs are in agreement with this statement, except the effect of the substrates on root N concentration. On the other hand, the results of no effect of substrate type and irrigation frequency on P concentrations in the tomato plant organs are in contradiction with previous published works (Silber and Bar-Tal, 2008; Silber et al. 2003; Xu et al. 2004). The substrate and the irrigation frequency had significant effects on Ca and Mg concentrations in part of the plants organs. The lowest concentration of Ca and Mg in the roots were obtained in the Perlite and the mixture of perlite with coir while the highest values were obtained in the Tuff and the Coir substrates. Irrigation frequency had significant effect on root Ca concentration, with mean values in low and high fertigation of 7.8 and 9.5 mg g-1, respectively. These results indicate that the limiting process for Ca uptake by the roots is the transport of Ca in the substrates to the roots, in agreement with published works reviewed by Silber and Bar-Tal (2008). In contradiction to the concentration of Mg in the roots the leaf Mg concentration was lower under high irrigation frequency, probably due to competition with Ca and dilution effect in the growing stem.

Table 13. Mineral composition (N, P and K) of plants organs as affected by substrate type and irrigation frequency in Experiment I at termination of growth, May 8th 2016, Ramat Negev, Israel.

a. Ca and Mg

Substrate	Irrigation frequency	Stem		Leaves		Fruits		Roots	
		Ca	Mg	Ca	Mg	Ca	Mg	Ca	Mg
		mg g^{-1}							
Coir	low	6.2	2.55	93.1	4.39	0.82	1.68	8.0	4.06
Coir	high	7.1	2.40	84.2	3.80	1.10	2.16	10.6	3.14
Perlite	low	4.1	2.13	39.7	4.27	1.44	1.41	6.9	2.59
Perlite	high	3.7	1.52	45.0	3.94	0.92	1.60	5.8	2.65
Perlite+Coir	low	4.8	2.29	52.3	4.25	0.70	1.86	6.0	3.30
Perlite+Coir	high	3.6	1.52	41.3	3.92	0.74	1.64	7.8	3.67
Tuff	low	5.5	1.92	102.9	4.12	0.93	2.13	9.3	3.81
Tuff	high	6.4	1.77	81.4	3.88	0.87	2.06	12.4	4.42
Tuff+Coir	low	7.0	2.17	46.4	3.99	0.91	1.85	8.7	4.02
Tuff+Coir	high	4.8	1.90	44.7	3.92	0.77	2.01	11.7	4.19
Variable	df	Prob > F							
substrate	4	0.056	0.254	0.070	0.828	0.088	0.274	0.002*	0.01*
irrigation	1	0.546	0.066	0.569	0.002*	0.450	0.414	0.019*	0.681
block	3	0.616	0.740	0.905	0.421	0.125	0.133	0.4430	0.326
substrate *Irrigation	4	0.523	0.805	0.979	0.713	0.173	0.580	0.3602	0.497

Table 13. Continued

b. N and P

Substrate	Irrigation frequency	Stem		Leaves		Fruits		Roots	
		N	P	N	P	N	P	N	P
		mg g^{-1}							
Coir	low	12.2	4.33	ND	ND	15.7	3.09	14.5	3.71
Coir	high	14.8	4.54	24.0	5.30	13.0	3.02	13.1	4.11
Perlite	low	13.7	4.71	25.4	5.62	11.1	3.76	17.5	3.23
Perlite	high	11.6	3.40	30.6	6.10	17.4	3.57	16.4	2.96
Perlite+Coir	low	13.1	3.97	28.1	3.61	19.1	4.01	13.7	2.75
Perlite+Coir	high	11.9	2.72	29.0	4.08	21.4	4.17	14.4	3.30
Tuf	low	12.0	3.03	27.6	4.26	19.7	3.77	16.0	3.54
Tuf	high	10.8	2.83	28.9	3.59	20.7	4.07	13.2	3.50
Tuf+Coir	low	13.2	3.66	26.2	4.55	24.7	4.88	10.9	2.74
Tuf+Coir	high	13.8	3.82	20.8	4.68	19.3	4.16	7.2	2.89
Variable	df	Prob > F							
substrate	4	0.527	0.128	0.742	0.109	0.175	0.399	0.006*	0.534
irrigation	1	0.907	0.256	0.470	0.605	0.871	0.965	0.162	0.672
block	3	0.857	0.551	0.934	0.178	0.595	0.241	0.863	0.408
substrate *Irrigation	4	0.438	0.496			0.666	0.947	0.788	0.960

Experiment II: October 2016 – March 2017

The second greenhouse trial was conducted between October 8th 2016 to March 20th 2017 in Ramat Negev Experimental Station. This experiment included three variables: substrate, irrigation frequency and container geometry. The tested substrates were: Tuff, Coconut Coir, Tuff/Coconut Coir (70%/30%) and Growstones. Each substrate was tested in two container geometries 47*25*30 cm and 48*50*15 cm (Length, Width, Height) of a constant volume of ≈350 l. Two irrigation frequencies (Low, High) were applied to each combination of substrate with container geometry (Table 14). The experimental design is of randomized 16 treatments in 3 blocks. Tomato transplant were planted on October 8th 2016 into the containers, 2 rows in each container, 40 cm between plants in row, the distance between rows varied with container geometry. Each container was irrigated with one line of drippers in the center of the container, parallel to the rows. The irrigation system consisted of laterals with integral drippers of 1.6 l/h line, 20 cm between drippers (one dripper for each plant), in the center of each container. Each plot was composed of three containers in a row. Drainage was collected from containers painted purple (Figure 34) and amount of water was measured and chemical analysis of drainage water was performed.

Table 14. Treatments of the second greenhouse trial that started on October 8, 2016.

Treatment	Medium	Irr. Freq.	Height
1	TUFF	Low	15
2	COIR	Low	15
3	TUFF+COIR	Low	15
4	Growstone	Low	15
5	TUFF	Low	30
6	COIR	Low	30
7	TUFF+COIR	Low	30
8	Growstone	Low	30
9	TUFF	High	15
10	COIR	High	15
11	TUFF+COIR	High	15
12	Growstone	High	15
13	TUFF	High	30
14	COIR	High	30
15	TUFF+COIR	High	30
16	Growstone	High	30

Figure 34: Second greenhouse trial at the Ramat Negev Experimental Station.

Air temperature and humidity in the greenhouse were monitored and recorded continuously through the experiment. Acclima sensors were inserted in the following treatments: First experiment - in six of the treatments (1, 2, 3, 6, 7, 8), three substrates (Tuff, Perlite and Coir) combined with the two irrigation frequencies (High and Low) at two depths (5 cm and 15 cm below top of the containers); Second experiment – in twelve of the treatments (1, 2, 3, 5, 6, 7, 9, 10, 11, 13, 14, 15), three substrates (Tuff, Coir and a mixture of Tuff + Coir) combined with the two irrigation frequencies (High and Low) at two containers heights (15 and 30 cm), at two depths in the tall containers (7.5 cm and 22.5 cm below top of the containers) and at 7.5 cm

below top of the containers in the short containers; Sensors were attached to data collector reading %water content, temperature and EC at 5 minutes intervals.

Tomato yield was monitored throughout the whole season by selective harvesting of ripe fruits from the central container of each plot, 1 to 3 times per week according to the ripening rate. The fruits were classified to quality standards and monitoring of physiological disorders. In Experiment I leaves samples were taken on November 24th 2015. Whole plant samples were taken twice, on December 31st 2015 and March 23rd 2016 and at the termination of the experiment (May 8th 2016, one plant per plot on the first two sampling dates and 3 plants at termination). In Experiment II whole plant samples were taken twice, on February 2017 and at the termination of the experiment (March 21st 2017, one plant per plot on the first sampling date and 3 plants at termination). Plant organs were dried (650C), fresh and dry weight were determined and subsamples were ground and digested with sulfuric acid for essential nutrients (N, P, K) analyses.

The maximum air temperature in the greenhouse during the main harvesting of fruits increased from a range of 22-24 °C in December 2016 to 30-34 in March 2017 (Fig. 35). The minimum temperature during these period increased from 3-5 OC in December 2016 to 10-12 in March 2017. Thus, the minimum air temperature was about 20 to 24 degrees lower than the maximum. Because the termination of the experiment was about 6 weeks earlier than in Experiment I, the growth period didn't include the late spring – early summer season period from April to May of very high maximum daily temperature, with a difference of 30 degrees between the maximum and minimum temperature. The maximum relative air humidity was in the range of 80 to 100 % throughout the harvesting time in experiment II with an average above 90%. These high humidity values were always obtained during night time. Whereas the minimum relative air humidity values were in a range of 25-45% with an average of 35%.

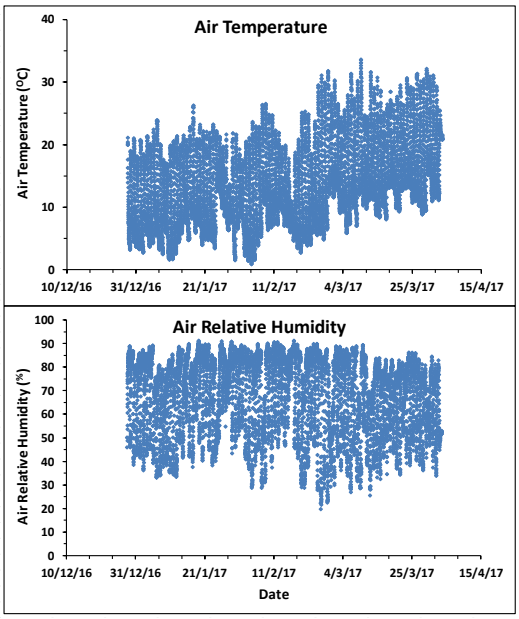

Figure 35: Air temperature and relative humidity during the tomato plant growth in the greenhouse, Experiment II, December 2016 to April 2017, Ramat Negev, Israel.

The effects of the substrate type (except the Growstones substrate), the geometry of the containers (15 and 30 cm height) and irrigation frequency on the dynamic of water content and temperature in the substrates were monitored continuously by TDT and TDR sensors (Acclima LTD) (Fig. 36). In the tall containers the sensors were positioned in two positions, 7.5 and 22.5 cm bellow the top surface of the containers. As expected the daily maximum and minimum volumetric water contents were considerably and consistently affected by the substrate type, with the highest values in the Coir (20 to 40%, 22.5 cm from the top) and the lowest in the Tuff (10 to 25%, 22.5 cm from the top), while the moisture content in the mixture of Tuff and Coir was just slightly higher than the pure Tuff. The water content in the deeper position, 22.5 cm bellow the top surface of the containers (or 7.5 cm above the bottom), was considerably higher than in the shallow position of 7.5 cm bellow the top surface of the containers (or 22.5 cm above the bottom), in agreement with the results of the previous year (Experiment I); For example, in the Coir the ranges of the daily minimum water contents were 25-30% and 10-20%, respectively. The minimum daily volumetric water contents were considerably affected by the irrigation frequency, much lower values were obtained in the low than high frequency irrigation, whereas the effect on the maximum daily values was small. The effect of irrigation frequency on the daily minimum water content was stronger in the tall than short containers comparing the 7.5 cm position. It should be noted that in this position the height above the bottom is 22.5 and 7.5 cm in the tall and short containers, thus in this position the water tension in the tall container is higher.

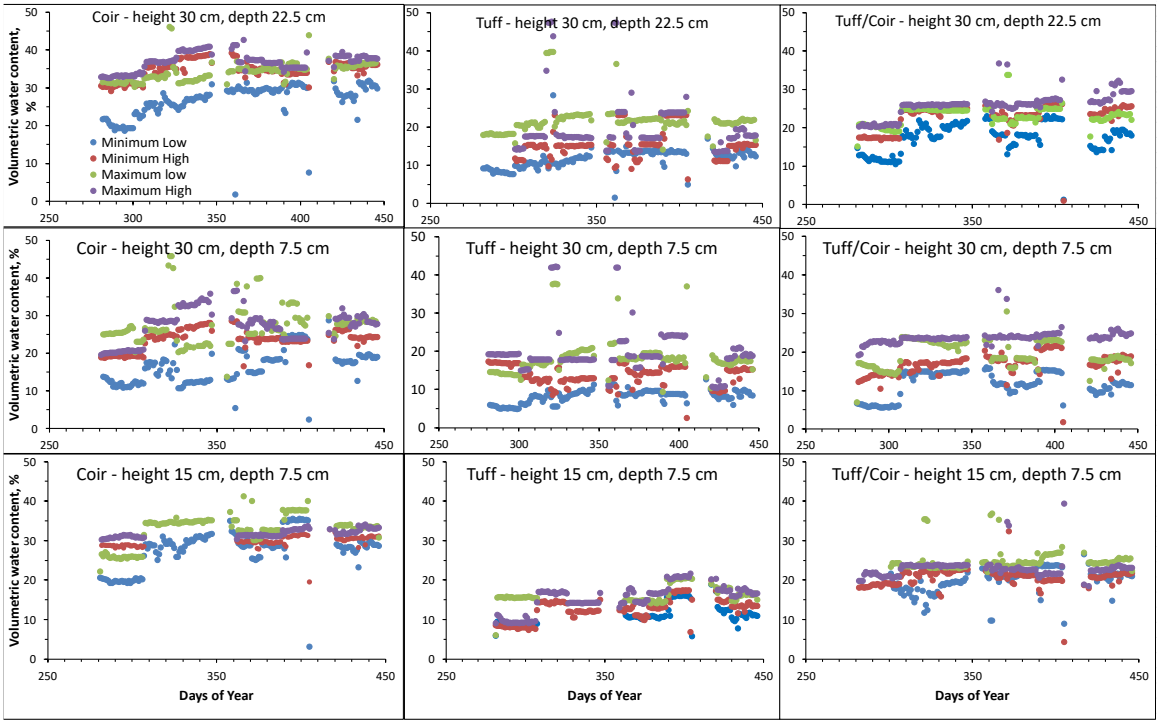

Figure 36a: The effects of the type of substrate, container height, irrigation frequency and the position of the sensors (at 7.5 and 22.5 cm below the containers surface) on the dynamic with time of volumetric water content (θ) in the growing medium, Experiment II, from October 7th 2016 to March 21th 2017, Ramat Negev, Israel.

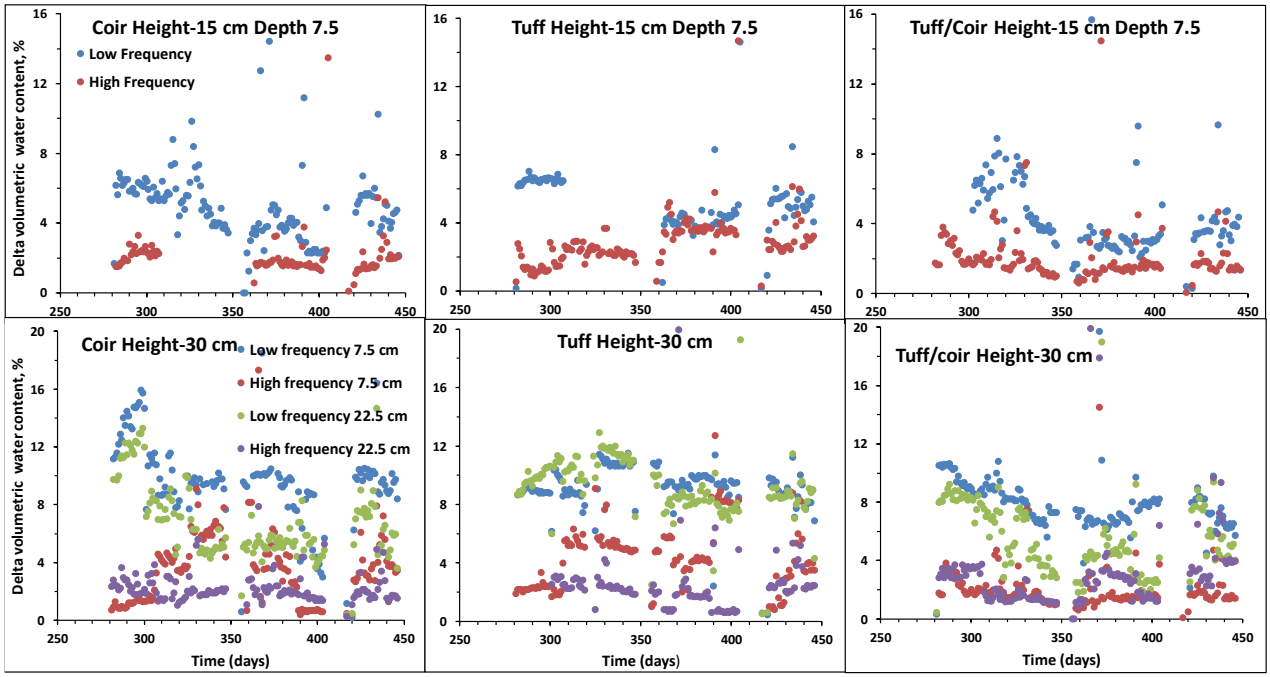

Figure 36b: The effects of the type of substrate, container height, irrigation frequency and the position of the sensors (at 7.5 and 22.5 cm below the containers surface) on the dynamic with time of the differences in water content between the daily maximum and minimum values (delta θ) in the growing medium, Experiment II, from October 7th 2016 to March 21th 2017, Ramat Negev, Israel.

The difference between the daily maximum and minimum water contents (delta θ), was considerably bigger under low than high irrigation frequency, in all studied substrates Coir, Tuff and Tuff/Coir mixture (Fig. 37). It should be noted that the substrate type had small effect on delta θ, although the maximum and minimum volumetric contents of Coir were considerably higher than in Tuff and the mixture of Tuff/Coir. As expected, delta θ was much bigger in the shallow position (7.5 cm bellow top) than the deeper position (22.5 cm bellow top). Thus, the mean delta θ in the tall containers is higher than in the short ones.

The temperature of the substrate showed considerable change with time, starting with maximum values of 25-27 oC at planting (October 2016), decreasing to minimum values of 8-10 oC in the end of December 2016 and increasing gradually to peak values of 25 oC at the termination of the experiment (March 21th 2017). No considerable effect of the type of substrate was obtained, in agreement with the measurements in Experiment I. The differences between the daily maximum to minimum temperature were very small in the deep position in the tall containers, whereas considerable differences of 5 to 7 ^{o}C were measured 7.5 cm bellow the top in the tall and short containers. Irrigation frequency had no considerable effect on temperature, in agreement with the results in Experiment I and in contradiction to the results of Heller et al (2015). However, in the current experiment in contrast to this of Heller et al (2015), the irrigating water system was well protected from direct sun light, therefore the water temperature was kept constant and moderate and irrigation events did not enhance the temperature of the substrate.

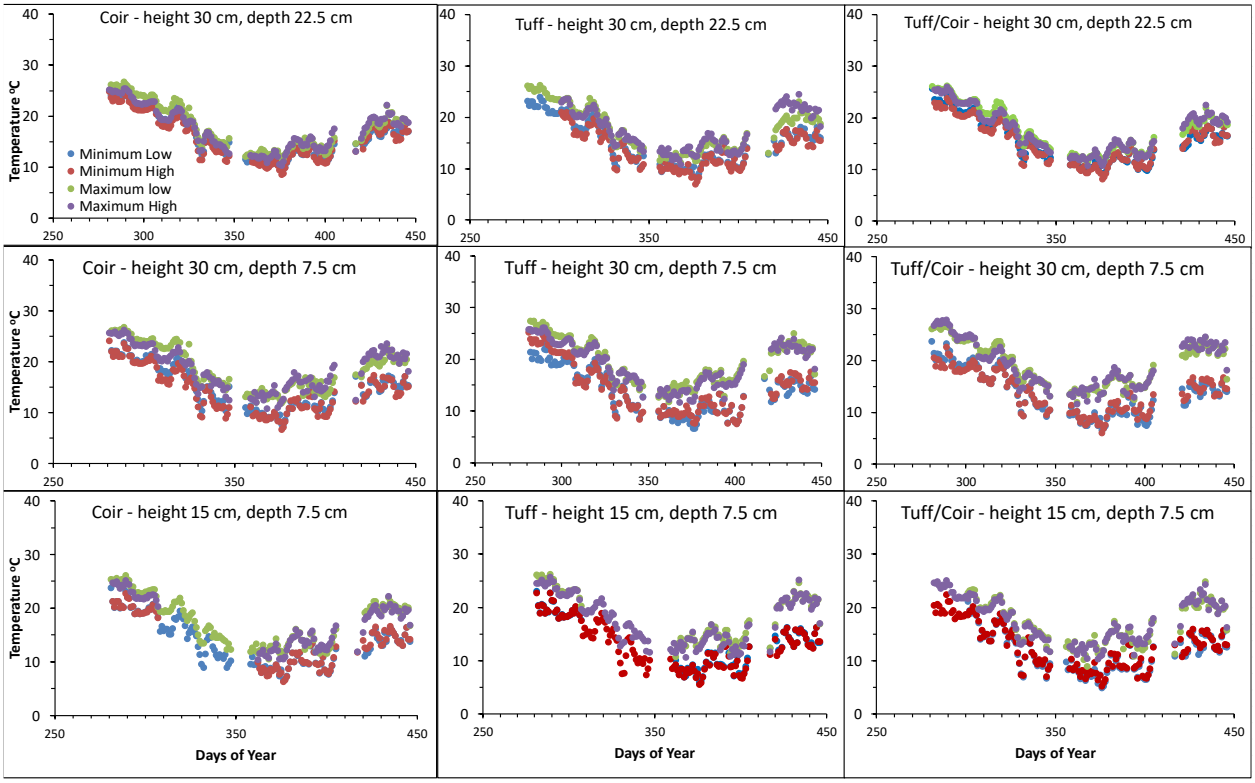

Figure 37: The effects of the type of substrate, container height, irrigation frequency and the position of the sensors (at 7.5 and 22.5 cm below the containers surface) on the dynamic with time of the differences in water content between the daily maximum and minimum values (delta θ) in the growing medium, Experiment II, from October 7th 2016 to March 21th 2017, Ramat Negev, Israel.

Total as well as high quality fruit yields were significantly affected by two factors, irrigation frequency and the containers height (Table 15 and Fig. 38). High irrigation frequency enhanced total and high quality fruit yields in agreement with published literature on the high sensitivity of plants grown in soilless culture to water availability and therefore the positive effect of frequent irrigation. The total and high quality fruit yields were higher in the tall than the short containers. This effect is in contradiction to the effect of the geometry of the container on the quality of lettuce (Heller et al. 2015), however, as we showed in the previous section the temperature of the substrate in the current experiment was not affected by the geometry of the container. On the other hand, it could be expected that the bigger mean delta θ in the tall containers will reduce the total fruit yield, at least when combined with low frequency irrigation. There were no significant interaction effects of irrigation frequency with container height on fruit yield and quality, but there was a trend of higher positive effect of high irrigation frequency in the tall than the short containers (Fig. 38). The substrate type had no effect on total and high quality fruit yields, however the occurrence of blossom end rot (BER) was higher in the Coir substrate than the other substrate. It is well proven that BER occurrence is enhanced by low availability of water and Ca. The water content in the Coir was higher than in the other

substrates, but there was no considerable difference in delta θ between the substrates. However, it should be noted that the occurrence of BER in the current experiment was relatively small, approximately 2.1% in the worst case, Coir substrate. The occurrence of other factors that caused fruit damage and deformation was higher in the short than tall containers. The effects of the irrigation frequency and the height of the containers on fruit yields started to appear in the middle of the winter, in the third week of January, about two months before termination of Experiment II. We assume that if the experiment could be maintained for longer period the differences between treatments would become bigger and more significant.

Table 15. Total fruit yield and quality parameters as affected by substrate type, container shape (15 and 30 cm height) and irrigation frequency, Experiment II, selective harvesting from 29.11.2016 to 21.3.2017, Ramat Negev, Israel.

Variable		Total yield	High quality Yield	BER	Other defected
		kg m^{-2}			
Substrate					
Coir		13.75	11.31	0.293 a	2.14
GrowStone		13.65	11.27	0.096 b	2.26
Tuff		13.58	11.65	0.083 b	1.83
Tuff/Coir		13.71	11.60	0.086 b	2.01
Irrigation frequency					
Low		13.04 b	10.89 b	0.18	1.97
High		14.30 a	12.03 a	0.10	2.16
Height					
15		13.03 b	10.62 b	0.14	2.25 b
30		14.32 a	12.29 a	0.14	1.87 a
Variable	df	Prob > F			
substrate	3	0.9942	0.9126	0.0029*	0.2225
Irrigation	1	0.0084*	0.0202*	0.0973	0.2088
height	1	0.0074*	0.0012*	0.9887	0.0132*
block	2	0.4978	0.7414	0.2130	0.4161
substrate *Irrigation	3	0.2198	0.2803	0.6965	0.8336
substrate *height	3	0.4682	0.5095	0.6694	0.2878
Irrigation *height	1	0.3829	0.8714	0.2092	0.0585
substrate *Irrigation *Height	3	0.7829	0.8890	0.5118	0.8907

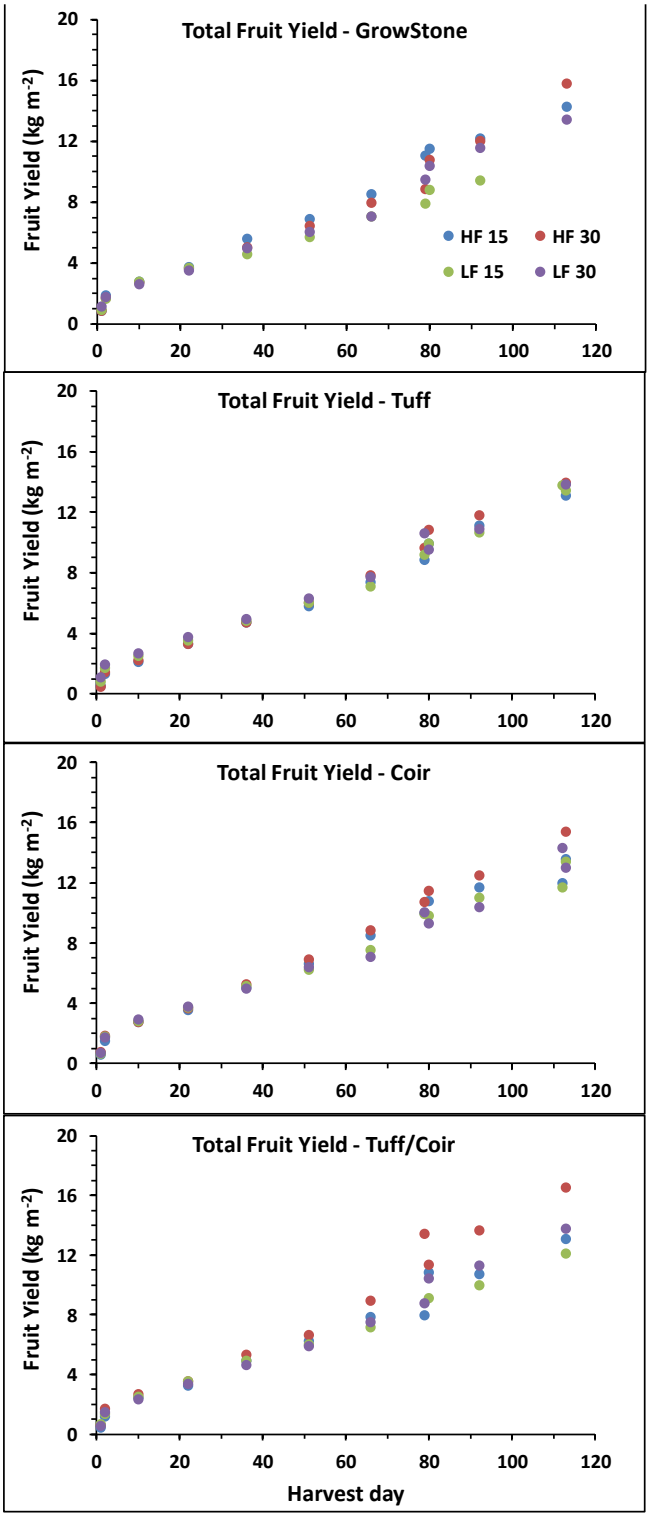

Figure 38: Total fruits yield as a function of time as affected by substrate type, container shape (15 and 30 cm height) and irrigation frequency, Experiment II, selective harvesting from 29.11.2016 to 21.3.2017, Ramat Negev, Israel.

References

Čereković, N., Todorović, M. and Snyder, R.L., 2010. The relationship between leaf area index and crop coefficient for tomato crop grown in southern Italy. Euroinvent, 1(1), pp.3-10.

Chamindu Deepagoda et al., 2012. Diffusion aspects of designing porous growth media for earth and space soils. Soil Sci. Soc. Am. J. 76, 1564–1578.

Durner, W., 1994. Hydraulic conductivity estimation for soils with heterogeneous pore structure. Water resources research, 30(2), pp.211-223.

Gee, G.W., M.D. Campbell, G.S. Campbell, and J. H. Campbell, 1992. Rapid measurement of low soil water potentials using a water activity meter, Soil Sci. Soc. Am. J., 56:1068-1070.

Hanson, B.R., Šimůnek, J., Hopmans, J.W., 2006. Evaluation of urea-ammonium nitrate fertigation with drip irrigation using numerical modeling. Agricultural Water Management 86, 102–113.

Hardelauf, H., M. Javaux, M. Herbst, S. Gottschalk, R. Kasteel, J. Vanderborght, and H. Vereecken, PARSWMS: a parallelized model for simulating 3-D water flow and solute transport in variably saturated soils, Vadose Zone Journal, 6(2), 255-259, 2007.

Heller, H., A. Bar Tal, S. Assouline, K. Narkis, S. Suryano, A. de la Forge, M. Barak, H. Alon, M. Bruner, S. Cohen and D. Tsohar. 2015. The effects of container geometry on water and heat regimes in soilless culture: lettuce as a case study. Irrig Sci. 33: 53–65.

Kempers, A.J. and Zweers, A., 1986. Ammonium determination in soil extracts by the salicylate method. Communications in Soil Science & Plant Analysis, 17(7), pp.715-723.

Kovar, J.L. and Pierzynski, G.M., 2009. Methods of phosphorus analysis for soils, sediments, residuals, and waters second edition. Southern cooperative series bulletin, 408.

Lieth and Oki, 2007. Irrigation in soilless production. In Raviv and Lieth (eds.) Soilless Culture – Theory and Practice. Elsevier Science, ISBN 9780444529756.

Reynolds, W.D., D.E. Elrick, E.G. Youngs, H.W.G. Booltink and J. Bouma. 2002. “Saturated and field-saturated water flow parameters: Laboratory methods.” In Methods of Soil Analysis, Part 4, Physical Methods (Ed., J.H. Dane and G.C. Topp). Soil Sci. Soc. of America, Madison, WI. p. 802-817.

Silber, A. and Bar-Tal, A. 2008. Nutrition of Substrates-Grown Plants. In: Soilless Culture: Theory and Practice. (M. Raviv and J.H. Lieth, eds.) p 291-339. Elsevier, The Netherlands

Silber, A., G. Xu, I. Levkovitch, S. Soriano, A. Bilu, and R. Wallach. 2003. High fertigation frequency: the effects on uptake of nutrients, water and plant growth. Plant and Soil 253: 467–47

Silber, A., I. Levkovitch, I. Dinkin, S. Soriano, M. Bruner, E. Kenig, G. Reshef, H. Zohar, I. Posalski, H. Yehezkel, D. Shmuel, S. Cohen, M. Dinar, E. Matan, and S. Assouline, 2005. High irrigation frequency and temporal NH4 concentration: the effects on soilless-grown bell pepper. J. Hortic. Sci. Biotech., 80:233-239.

Šimůnek et al., 2012. The HYDRUS Software Package for Simulating the Two- and Three-Dimensional Movement of Water, Heat, and Multiple Solutes in Variably-Saturated Porous Media – Technical Manual, University of California Riverside, Riverside, CA.

Šimůnek, J., K. Huang, and M. Th. van Genuchten, The SWMS_3D code for simulating water flow and solute transport in three-dimensional variably saturated media, Version 1.0, Research Report No. 139, U.S. Salinity Laboratory, USDA, ARS, Riverside, California, 155 pp., 1995.

Thompson et al., 2007. Using plant water status to define threshold values for irrigation management of vegetable crops using soil moisture sensors. Agric. Water Manag. 88, 47–158.

Tuller, M., and D. Or, 2004. Water retention and characteristic curve. In D. Hillel (Ed.), Encyclopedia of Soils in the Environment - Volume 4, Elsevier Ltd., Oxford, U.K., pp.278-289.

van Dam, J.C., Huygen, J., Wesseling, J.G., Feddes, R.A., Kabat, P., van Valsum, P.E.V., Groenendijk, P., van Diepen, C.A., 1997. Theory of SWAP, Version 2.0. Simulation of water flow, solute transport and plant growth in the Soil- Water-Atmosphere- Plant environment. Department of Water Resources, WAU, Report 71, DLO Winand Staring Centre, Wageningen, Technical Document 45.

van Genuchten, M.T., 1980. A closed-form equation for predicting the hydraulic conductivity of unsaturated soils 1. Soil science society of America journal, 44(5), pp.892-898.

van Genuchten, M.Th., 1987. A numerical model for water and solute movement in and below the root zone. Research Report No. 121, U.S. Salinity Laboratory, USDA, ARS, Riverside, CA.

Vrugt, J.A., Hopmans, J.W., Šimůnek, J., 2001. Calibration of a two-dimensional root water uptake. Soil Sci. Soc. Am. J. 65, 1027–1037.

Xu, G., I. Levkovitch, S. Soriano, R. Wallach, and A. Silber, 2004. Integrated effect of irrigation frequency and phosphorus level on lettuce: yield, P uptake and root growth. Plant Soil 263: 297-309.

Publications for Project IS-4764-14R

Status	Type	Authors	Title	Journal	Vol:pg Year	Coun
Published	Abstract - Poster	*Gohardoust, M.R., T.P.A. Ferre, A. Bar-Tal, H. Heller, M. Amichai, and M. Tuller*	Optimization of Soilless Greenhouse Substrates Based on Physicochemical Characterization and Numerical Simulations	***ASA-CSSA-SSSA International Annual Meeting***	: 2015	Joint
Published	Abstract - Poster	*Gohardoust, M.R., J. An, A. Bar-Tal, H. Heller, M. Amichai, T.P.A. Ferre, and M. Tuller*	Application of Numerical Simulations for Optimization of Soilless Culture Systems	***ASA-CSSA-SSSA International Annual Meeting***	: 2016	Joint
Published	Abstract - Poster	*Gohardoust, M.R., H. Hardelauf, A. Bar-Tal, H. Heller, M. Amichai, and M. Tuller*	Application of the PARSWMS Parallelized Code for Simulation of Three-Dimensional Water Flow and Solute Transport in Containerized Soilless Substrates	***ASA-CSSA-SSSA International Annual Meeting***	: 2017	Joint
Published	Abstract - Poster	*Gohardoust, M.R., A. Bar-Tal, and M. Tuller*	Hydraulic and Aeration Properties of Soilless Greenhouse Substrate Mixtures	***SSSA International Soils Meeting***	: 2019	Joint
Published	Book Chapter	*Bar-Tal, A., U.K. Saha, M. Raviv, and M. Tuller*	Inorganic and Synthetic Organic Components of Soilless Culture and Potting Mixtures	***Soilless Culture, Second Edition***	: 2019	Joint